

# Empirical Analysis of EIP-1559: Transaction Fees, Waiting Time, and Consensus Security

Yulin Liu  
SciEcon CIC  
Bochsler Finance  
Switzerland

Yuxuan Lu  
Center on Frontiers of Computing  
Studies  
Peking University  
China

Kartik Nayak  
Department of Computer Science  
Duke University  
USA

Fan Zhang\*  
Department of Computer Science  
Duke University  
USA

Luyao Zhang\*  
SciEcon CIC  
Data Science Research Center and  
Social Science Division  
Duke Kunshan University  
China

Yinhong Zhao<sup>†</sup>  
SciEcon CIC  
Department of Economics  
Duke University  
USA

## ABSTRACT

Transaction fee mechanism (TFM) is an essential component of a blockchain protocol. However, a systematic evaluation of the real-world impact of TFMs is still absent. Using rich data from the Ethereum blockchain, mempool, and exchanges, we study the effect of EIP-1559, one of the first deployed TFMs that depart from the traditional first-price auction paradigm. We conduct a rigorous and comprehensive empirical study to examine its causal effect on blockchain transaction fee dynamics, transaction waiting time, and security. Our results show that EIP-1559 improves the user experience by making fee estimation easier, mitigating intra-block difference of gas price paid, and reducing users' waiting times. However, EIP-1559 has only a small effect on gas fee levels and consensus security. In addition, we found that when Ether's price is more volatile, the waiting time is significantly higher. We also verify that a larger block size increases the presence of siblings. These findings suggest new directions for improving TFM.

## KEYWORDS

EIP-1559, transaction fees, waiting time, consensus security, empirical analysis

## 1 INTRODUCTION

Computation and storage on public blockchains such as Bitcoin and Ethereum are scarce resources [15]. To allocate blockchain resources to users, a transactions fee mechanism (TFM) needs to be employed. TFM is an essential component of a blockchain protocol that can fundamentally affect incentive compatibility, user experience, and security of a blockchain system [26, 28, 34, 61]. Ethereum, for example, used to employ first-price auctions as the transaction fee mechanism [68].

While many have proposed novel TFMs beyond simple first-price auctions [12, 28, 41, 64, 73], there has not been a real world

implementation until the Ethereum Improvement Proposal 1559 (EIP-1559) [62] on Ethereum, the second largest blockchain network in market capitalization to date.

On August 5th, 2021, Ethereum activated a major upgrade named London Hardfork [31], which implemented EIP-1559 together with several other EIPs and overhauled the Ethereum TFM. EIP-1559 introduced several novel elements while maintaining backward compatibility. Notably, for instance, it includes a base fee parameter that indicates the minimum gas price users need to pay in each block, which adjusts dynamically according to the gas used in the previous block. It also changes how users specify transaction fee bids. We defer more details on EIP-1559 to Section 3.

To the best of our knowledge, EIP-1559 is not only the first major TFM change on Ethereum but also the first real attempt to depart from first-price auctions on any major blockchain. The impact of this upgrade is profound. Multiple prior works have examined EIP-1559 from a theoretical point of view. Roughgarden [68] gives a thorough game-theoretical evaluation on EIP-1559 mechanism and pointed out its incentive compatibility for myopic miners. Reijbergen et al. [64] observed the volatile gas usage after EIP-1559 and proposed modifications to mitigate this issue. The Ethereum community had analyzed the EIP informally [16, 56] and expected the upgrade to mitigate the economic inefficiencies due to fee volatility, to avoid over-paid transaction fees, and to lower transaction waiting time [62]. However, the real-world impact of a novel TFM such as EIP-1559 has not been systematically studied.

We aim to close this gap with a comprehensive and rigorous empirical study. As a major and probably the only recent TFM reform, EIP-1559 presents a unique opportunity to study the causal effects of TFM changes on blockchain characteristics. While we focus on Ethereum, the insight we gain can generalize to other blockchains and future TFM reforms. We aim to answer three questions on the impact of this TFM reform.

- Does EIP-1559 affect the transactions fee dynamics? Existing theoretical studies predict an easier fee estimation in the novel TFM because the Symmetric Ex-post Equilibrium (SEE) is easier to solve than the Bayesian Nash Equilibrium (BNE) in the previous first-price auction for bounded rational users. [28, 68]. However,

\*Corresponding authors:

Fan Zhang (email:fanz@cs.duke.edu, address: Duke University, 308 Research Dr, Durham, NC 27705, United States) and Luyao Zhang (email:lz183@duke.edu, address: Duke Kunshan University, No.8 Duke Ave, Kunshan, Jiangsu 215316, China.)

<sup>†</sup>The authors are listed in alphabetical order according to last name, and they contributed equally to this work.

the rationality of users on Ethereum is yet to be tested. Thus, it’s essential to verify the theoretical implications empirically.

- Does EIP-1559 affect transaction waiting time? Ethereum community expects the TFM to lower transaction delay [16], but it is unclear yet whether and how this happens.
- Does EIP-1559 affect consensus security? EIP-1559 introduces significant changes to the block size (in terms of gas used) and the incentive system of miners and users. The security implications are widely debated [17, 56], but little real-world evidence is known. We aim to settle the arguments through empirical evidence.

## Challenges and our approach

To answer these questions, we collected rich data from Ethereum blockchain, mempool<sup>1</sup> (for computing waiting time), and exchanges (e.g., intra-day ETH prices) [50, 60]. The measurements of many blockchain characteristics are challenging. For example, measuring the waiting time of transactions requires accurate observations of the mempool. We set up a distributed data collection system to monitor the mempool of Ethereum and capture the timestamps when each transaction is submitted to the mempool, thus obtaining a precise measure of transaction waiting time.

Empirically, it would be difficult to separate the effect of EIP-1559 on blockchain characteristics with other confounding factors, such as price volatility, network instability, and time trend. An empirical study aiming at unbiased estimates must control these confounding factors. Thus, we adopt an event study [51] and regression discontinuity design (RDD) [9, 43] framework that enables the estimation of causal effects. By comparing observations of data on either side of the London Hardfork, we estimate the local average treatment effect of EIP-1559.

## Our Findings

**Transaction fees.** We observe that EIP-1559 did not lower the transaction fee level itself in our data period, but it enabled easier fee estimation for users.

Before EIP-1559, users pay the entirety of their bids, so they risk *overpaying* transaction fees if the network condition turns out less congested after they bid. With the new TFM, however, such risks are avoided, because users can set two parameters in their bids: a cap on the total fees they will pay per gas (called “max fee per gas”) and a tip for the miner on top of the base fee (called “max priority fee per gas”). The actual fee paid is either the max fee per gas or the sum of the base fee and the max priority fee per gas, whichever is smaller. More details of EIP-1559 will be provided below in Section 3.3.

This separation enables a simple yet optimal bidding strategy (dubbed obvious optimal bid in [68]) where users just set the max fee per gas to their intrinsic value for the transaction and set the max priority fee per gas to the marginal cost of miners. As we will elaborate in Section 5.2, we observe that the bids users submit after EIP-1559 are consistent with this obvious optimal bid. We also observe that users who adopt EIP-1559 bidding pay a lower fee than those who stick to the legacy bidding. Both findings imply that fee

estimation is easier with the new gas fee bidding style. Moreover, our regression discontinuity analysis in Section 5.2.2 indicates that the intra-block gas price variance, measured by standardized inter-quartile range (IQR), becomes significantly lower as more users adopt EIP-1559 transactions. Therefore, the variance of intra-block gas prices decreases with EIP-1559, which also implies easier fee estimation and less overpaying for users. Our results thus advise future mechanism designers to consider the bounded rational players and design mechanisms easier for users to understand.

**Transaction waiting time.** We observe that EIP-1559 lowers transaction waiting time, thus improving the user experience.

We define waiting time as the difference between the time when we first observe the transaction in mempool and when the transaction is mined. Waiting time determines the latency of the commit. Moreover, when there are dependent transactions, users cannot submit new transactions until previous dependent transactions are successfully included in blocks or canceled. Thus, the delay has an opportunity cost associated with it.

We find that waiting time significantly reduces after London Hardfork possibly as a result of easier gas price bidding and variable-sized blocks. This benefits both the transactions that adopt the new bid style and the ones that still adopt legacy bidding. Thus, EIP-1559 improved the waiting time for transactions even though not all users have adopted it. The reduction in waiting time might also be a consequence of the easier fee estimation after EIP-1559. The true value of bidding reveals the opportunity cost of time. With a more obvious optimal bidding strategy, more urgent users bid higher to have their transactions included in the next available block.

**Consensus security.** EIP-1559 changes important consensus parameters such as the block size and the incentive of miners and users. To understand its impact on consensus security, we identified three possible avenues through which the EIP might affect consensus:

- *Fork rate.* Larger blocks may take more time to propagate through the p2p network leading to more forks [22, 65]. However, in EIP-1559 the block size is variable and dynamically adjusted, thus its impact on fork rate is not well understood. Our results empirically show that London Hardfork increased block size on average, and it also led to an about 3% rise in fork rates.
- *Network load.* We define network load as the amount of computational, networking, and storage work a node must perform to participate in the blockchain protocol. The community debated over whether variable block sizes will increase the network load [16, 17], since processing larger blocks consumes more resources. Our results show that EIP-1559 does not put the blockchain system under a significantly higher load for an extended period. We do observe load spikes—periods during which an above-average amount of gas is consumed—but its frequency is not significantly different before or after the London fork.
- *Miner Extractable Value (MEV [23]).* MEV refers to the profit a miner can make through their ability to arbitrarily include, exclude, or re-order transactions within the blocks they produce. Daian et. al. [23] pointed out that significant MEV can incentivize miners to deviate from the consensus protocol (e.g., to fork, or even rewind the blockchain to collect the profit in MEV [23]), thus destabilizing consensus. Through our empirical analysis, we

<sup>1</sup>On Ethereum, mempool is where transactions stay after sent by users and before being added to a block by miners.

find that MEV becomes a much larger share of miners’ revenue after EIP-1559, mainly because the base fees are burnt. This might create an incentive for miners to invest more in MEV extraction.

The rest of the paper is organized as follows. Section 2 reviews the related works in three lines of literature. Section 3 introduces the backgrounds and details of the EIP-1559 upgrade. Section 4 introduces our data sources, which we use in Section 5 to derive our empirical results. Section 6 discusses the results and concludes.

## 2 RELATED WORKS

This paper is related to three lines of literature: transaction fee mechanism design, waiting time modeling in market design, as well as consensus security.

### 2.1 Transaction Fee Mechanism Design

Since EIP-1559 was proposed, four recent papers have specifically investigated the proposal from different theoretical perspectives. Roughgarden (2021) [61] provides a general framework for transaction fee mechanism design and proves that the EIP-1559 mechanism has incentive compatibility for myopic miners and off-chain agreement proofness. That is to say, myopic miners have incentives to act along with the allocation rules and that no off-chain agreement or collusion can give a higher return for miners. Other than these results, Roughgarden (2020) [68] also analyzes the transaction fee and waiting time characteristics of EIP-1559 and points out that while no transaction fee mechanism can substantially lower transaction fees, EIP-1559 should lower the variance in transaction fees and waiting time through the flexibility of variable size blocks. The paper also argues that EIP-1559 does not weaken the system security regarding several types of attacks. Leonardos et al. [45] put the EIP-1559 mechanism in a dynamic system framework and study the stability of the system. They show that the base-fee adjustment parameter is critical to system stability and provide threshold bounds for the adjustment parameter. Reijdsbergen et al. [64] finds that block sizes have intense and chaotic oscillations after London Hardfork, which they believe could lead to harder fee estimation, and proposes an additive increase and multiplicative decrease (AIMD) fee adjusting model that can mitigate the spikes of block gas used.

Our work contributes to a growing set of economics and computer science literature on blockchain transaction fee mechanism design. The white paper of Bitcoin [53] proposes the first-price auction mechanism for the Bitcoin Payment System (BPS), which is later widely adopted by other early blockchains (e.g., Ethereum before London Hardfork, Litecoin). Several papers analyze the supply and demand equilibrium of the BPS fee dynamics [36, 38, 58, 66, 72], while others analyze the game-theoretical equilibrium [25]. Alternative mechanisms for transaction fees were also proposed. For example, Lavi et al. [41] and Yao [73] propose a monopolistic price mechanism where all transactions in the same block pay the same transaction fee, determined by the smallest bid. This approach is akin to the second-price auction. Basu et al. [12] propose Stable-Fees, a mechanism also based on second-price auction with a more realistic model of miner behavior. Ferreira et al. [28] propose a modification to EIP-1559 based on a dynamic posted-price mechanism that achieves more stability than EIP-1559 by their analysis.

Li [48] proposes a general concept of obviously strategy-proof (OSP) mechanisms that gives the rationale for providing more obvious mechanisms. Zhang and Levin [75] further provide a decision theory foundation for the OSP mechanism for bounded rational players.

### 2.2 Waiting Time Modeling in Market Design

Long waiting time and high transaction costs are major issues caused by network congestion, which is directly related to the scalability of blockchain [21, 33]. Easley, O’Hara, and Basu [26] provide a game-theoretical model of the BPS with an important complication on mempool queuing that relates user welfare to fee levels and waiting time. Huberman, Leshno, and Moallemi [37] further link the BPS to monopoly pricing of miners and suggest a protocol design of adjustable system parameters for efficient congestion pricing, which coincides with the idea of EIP-1559. Waiting time auctions and market designs to minimize frictions have been extensively studied in economics and operation research [35, 55, 67]. It is crucial to shorten waiting time by research in consumer psychology [40, 42] and the nature of many DeFi practices on blockchain [34].

While waiting time (delay) is widely used in the theoretical models of users’ utility function, few have found an effective way to measure and analyze it in the blockchain setting directly. Some use an external data source on waiting time and mempool size that is only available for Bitcoin [26]; others use block size or fee levels as proxies for network congestion [37, 69]. Azevedo Sousa et al. [10] use a similar approach with our paper by directly observing the mempool of Ethereum, but their data suffer from the problem of negative waiting time because of network latency. Our paper solves this problem by using the timestamp of the next block after the transaction concerned is included.

### 2.3 Consensus Security

The security of blockchain systems has been widely discussed since their inception [49]. Several papers analyzed the incentive system of the Bitcoin system and proposed potential attacks given specific incentive incompatibilities [18, 27, 44, 46, 59, 71]. Other studies extend the analysis to Proof-of-Stake protocols [20, 54].

Frequency of uncle blocks is an important indicator of blockchain forks which endanger network security. Uncle blocks in the Ethereum community refer to blocks submitted for a block height after that block height is finalized and miners have moved to the next block height. Ethereum adopts a variation of Greedy Heaviest Observed Subtree (GHOST) design [14, 70] that also provides block rewards to the miners of uncle blocks. Previous studies on Bitcoin show that a larger block size leads to longer propagation time, making it more likely for some miners to submit an uncle block [24, 70]. A higher uncle rate can lead to less network resilience to double-spend attacks and selfish mining, thus endangering consensus [32].

Daian et al. [23] firstly introduce the potential impact of MEV on security. Many works analyzed the MEV extraction in various blockchain infrastructures [7, 8, 11]. Chen et al. [19] investigated and systematized the vulnerabilities, attacks, and defenses of the Ethereum system security. Qin, Zhou, and Gervais [63] quantified the specific value of MEV and provided evidence that mining pools

are extracting MEV themselves. In early 2021, the inception of Flashbots made it easier to extract MEV and observe MEV extraction. In just a few months, the adoption rate of Flashbots increased rapidly, which was above 95% at the time that this paper was written [29]. More MEV extraction tools and protocols have appeared recently, including Eden network, Taichi network, [4, 5] etc.

### 3 BACKGROUND

#### 3.1 Transaction Fees in Ethereum

It takes bandwidth, computational, and memory resources to successfully execute operations on the Ethereum network [15]. The amount of resource consumed is measured in the unit of gas. For example, it costs 21,000 gas to send a transaction and 53,000 gas to create a smart contract.<sup>2</sup> To prevent malicious users from spamming the network or deploying hostile infinite loops, every operation is charged a fee [14]. The gas fee is paid in Ether,<sup>3</sup> dubbed ETH, the native currency of the Ethereum network, and calculated as:

$$\text{GasFee} = \text{GasUsed} \times \text{GasPrice}$$

Sending a transaction could trigger a series of other operations on the Turing-complete blockchain. Therefore, the amount of gas needed for a transaction is usually unknown before execution. To avoid the undue gas consumption, users could specify a gas limit with their transactions. Unconsumed gas is refunded. Ethereum has a block gas limit, 15 (30) million before (after) the implementation of EIP-1559. The sum of the gas limit of transactions included in a block cannot exceed this block gas limit. In the following two subsections, we explain the GasPrice in the above equation before and after the London Hardfork.

#### 3.2 Transaction Fee Mechanism prior EIP-1559

The legacy transaction fee mechanism before EIP-1559 is essentially a first-price auction. Users submit a gas price bid for their transactions to outbid competitors. Miners are incentivized to include those with the highest gas prices in a block first. However, the first-price auction does not have a Bayesian-Nash equilibrium [52], so users need to make assumptions on their competitors' bids to optimize their bid strategy, which is impractical and user-unfriendly. Besides, bidding leads to distorted resource allocation, such as overpaid and volatile gas fees, unduly long inclusion time of transactions, etc., which we will examine later. To resolve these issues, a new gas fee mechanism was proposed, discussed, and implemented as EIP-1559.

#### 3.3 The new TFM in EIP-1559

EIP-1559 [31] introduces four major changes to the transaction fee mechanism on Ethereum. A list of notations related to EIP-1559 is presented in Table 1.

**Block Size.** EIP-1559 changes the fixed-sized blocks to variable-sized blocks. The block gas limit is doubled from 15 million to 30 million, while the block gas target is still set at 15 million. As we will introduce below, a novel gas price mechanism ensures that block gas used remains around block gas target on average.

**Base Fee.** EIP-1559 introduces a base fee parameter determined by network conditions. Base fee is the minimum gas price that every transaction must pay to be included in a block. Base fee adjusts in a dynamic Markov process according to the block gas used in the previous block. If the block gas is greater than the target, the base fee for the next block increases, and vice versa. The base fee of the next block is determined solely by its present state. The dynamics of the base fee is represented as follows:

$$\text{BaseFee}_{h+1} = \text{BaseFee}_h \left( 1 + \frac{1}{8} \frac{\text{GasUsed}_h - \text{GasTarget}}{\text{GasTarget}} \right). \quad (1)$$

Here,  $h$  refers to the block height.  $\text{BaseFee}_h$  and  $\text{GasUsed}_h$  refer to the base fee and the block gas used in block  $h$ .  $\text{GasTarget}$  is fixed at 15 million.

**User Bidding.** The way users bid is modified in a backward-compatible manner. Users can optionally bid two parameters in their transactions, max priority fee per gas and max fee per gas. Priority fees per gas are the tips with which users incentivize miners to prioritize their transactions. Max fees are the fee caps users will pay including both base fees and priority fees. The difference between the max fee and the sum of the base fee and priority fee, if any, will be refunded to the user. The actual GasPrices of these transactions are calculated by:

$$\text{GasPrice} = \min\{\text{BaseFee} + \text{MaxPriorityFee}, \text{MaxFee}\}.$$

For example, if a user bids  $(\text{MaxFee}, \text{MaxPriorityFee}) = (60, 2)$ , then there can be several cases depending on the level of base fee in the current block:

- (1) If  $\text{BaseFee} > 60$ , the transaction must not be included in this block. It waits in the mempool until base fee falls.
- (2) If  $58 < \text{BaseFee} < 60$ , the miner can choose whether to include this transaction. If the transaction is included, then aside from the base fee, the user pays  $60 - \text{BaseFee}$  Gwei as a priority fee to miners. Users pay 60 Gwei per gas in total.
- (3) If  $\text{BaseFee} < 58$ , the miner can choose whether to include this transaction. If the transaction is included, aside from the base fee, the user pays 2 Gwei as a priority fee to miners. Users pay  $\text{BaseFee} + 2$  Gwei per gas in total.

It is worth noting that users are allowed to follow the legacy bid style and only bid a gas price, in which case the difference between gas price and base fee are all taken by miners as tips.

**Miners' Revenue.** The base fee is burned, while the priority fee is rewarded to the miners. Before EIP-1559, miners earn all gas fees in a block. With EIP-1559 implemented, tips are de facto mandatory because miners do not earn the base fee and otherwise they may mine empty blocks. Miners' revenues mainly include static rewards,<sup>4</sup> priority fees in the block, and uncle rewards if they mine an uncle block. In addition, miners also receive profits extracted from including, omitting, ordering, and inserting transactions, known as Miners Extractable Value (MEV) [23].

<sup>2</sup>See Appendix G of Ethereum Yellow Paper, <https://ethereum.github.io/yellowpaper/paper.pdf>.

<sup>3</sup>Gas price is usually measured in Gwei and 1 Gwei =  $10^{-9}$  ETH.

<sup>4</sup>The static reward is 2 Ether per block after the Constantinople Fork in February 2019 [30].

Notation	Description
BaseFee	The minimum GasUsed multiplier required for a transaction to be included in a block. The result of BaseFee times GasUsed is the part of the transaction fee that is burned
MaxPriorityFee	The maximum GasUsed multiplier that a user is willing to pay to the miner
MaxFee	The maximum GasUsed multiplier that a user is willing to pay for a transaction
GasPrice	Only legacy transactions use it, which represents the GasUsed multiplier that a user is willing to pay for a transaction
GasUsed	The total amount of gas used by a transaction
GasTarget	The target of gas that blocks are expected to use on average, which is set by the protocol
GasFee	The actual transaction fee that a user pays

Table 1: Notations related to EIP-1559

## 4 DATA

### 4.1 Data Sources and Metadata

We use three data sources. First, we query the blockchain data from Google Bigquery, which documents the block-level characteristics and transaction-level characteristics from Ethereum [60]. Second, we run four Ethereum full nodes geographically distributed around the world (North Carolina, Los Angeles, Montreal, and Germany) to monitor the mempool of Ethereum constantly, so we can capture a historical log of Ethereum mempool. Most users submit their transactions to mempool so that miners can consider their transactions.<sup>5</sup> The data fully captures the submission of each awaiting transaction in the mempool, including the time when they submitted and the bids on gas prices. It is worth mentioning that Ethereum mempool data is ephemeral, so our data is not reproducible at a later time. Third, we query ETH price data at a one-minute granularity from Bloomberg Terminal [50]. We use this data to compute minute level price volatility of ETH price as a control variable, which is an instrument for demand for transactions on Ethereum. A data dictionary can be found in Appendix A.

The time of our data is specified in Fig. 1. For the pre-London-Hardfork period, we use data from block number 12895000 (2021-07-20) to 12965000 (2021-08-05, the block of London Hardfork). For the post EIP-1559 period, we use data from block number 13035000 (2021-08-16) to block number 13105000 (2021-08-31). We do not use data from the blocks immediately after EIP-1559 because it takes time for users and miners to upgrade their software to adapt to the London Hardfork change. The Start Block of the post-EIP 1559 period is chosen when the adoption reaches 20%. We did not record mempool data between 2021-08-05 and 2021-08-16.

<sup>5</sup>Flash bots bundles and other private transactions may go around mempool, but they occupy a very small portion of transactions.



Figure 1: Periods and Block Numbers

### 4.2 Transaction Fee Data

We obtained blockchain data including the gas price paid for each transaction (legacy and EIP-1559) and the max fee and max priority fee bids for each EIP-1559 transaction from Google Bigquery [60].

From transaction-level data, we derive several block-level metrics. To measure the gas price of a “representative transaction” in the block, we use the median of gas prices from all transactions. Measuring the “variation” of gas prices in the block is somewhat trickier since there are outliers. Standard measures such as mean and standard deviation can be misleading and statistically meaningless. However, measures like median and inter-quartile range (IQR) are much more robust to outliers that we encounter frequently in blockchain data. We use the standardized IQR of gas prices in blocks to measure intra-block variance of gas prices, defined as

$$\text{standardized IQR} = \frac{Q_{75}(\text{GasPrice}) - Q_{25}(\text{GasPrice})}{Q_{50}(\text{GasPrice})}$$

where  $Q_{25}$ ,  $Q_{50}$ ,  $Q_{75}$  refer to the 25th, 50th, and 75th percentile of gas prices paid in a specific block. In addition, our data include block-level blockchain data such as miner’s block timestamp, base fee per gas, block gas used, block size, etc.

### 4.3 Waiting Time Data

We define the waiting time of a given transaction TX as the time the transaction waits in the mempool, namely

$$\text{Waiting time of TX} = T_{\text{block}}^{\text{TX}} - T_{\text{mempool}}^{\text{TX}}$$

where  $T_{\text{mempool}}^{\text{TX}}$  is the time when the transaction *first* appears in the mempool and  $T_{\text{block}}^{\text{TX}}$  is the time when the transaction is mined.

**Estimating  $T_{\text{mempool}}^{\text{TX}}$ .** Obtaining an exact  $T_{\text{mempool}}^{\text{TX}}$  is challenging because that would require monitoring the traffic of all (or most) P2P nodes. To obtain a reasonable approximation, we placed probing nodes across the globe to get representative samples of the mempool. Specifically, we modified the Ethereum Geth client [1] so that our nodes connect to up to 1,000 peers. We deployed 4 geographically distributed nodes in Durham, Los Angeles, Montreal, and Helsinki. Our modified Geth client stores a log of mempool whenever they receive a new transaction from the P2P network. We use the earliest time when TX is observed in mempool across all servers as the estimate of  $T_{\text{mempool}}^{\text{TX}}$ . Though we made various efforts to improve the accuracy of the mempool observations by placing probing nodes in different locations, increasing their connectivity, connecting to well-known nodes such as established mining pools [47], we note that the estimation may not be perfect. Further improving the mempool observation could be an interesting future work.

**Estimating  $T_{\text{block}}^{\text{TX}}$ .** As defined above,  $T_{\text{block}}^{\text{TX}}$  is the time when the transaction appeared in a block. One may attempt to set  $T_{\text{block}}^{\text{TX}}$  to the

block timestamp given by miners, but that is vastly inaccurate. For instance, Azevedo-Sousa et al. [10] calculated waiting time in this fashion which led to the wrong conclusion that 50% of transactions have *negative* waiting times! The reason is that block timestamps given by miners are typically when the miner *starts* the mining process, whereas  $T_{\text{block}}^{\text{TX}}$  is when the mining process *ends*.

Obtaining a precise  $T_{\text{block}}^{\text{TX}}$  would require monitoring the traffic of all (or most) miners, which is very challenging. We bypass this difficulty by using the timestamp of the *next* block (i.e., the block after the one in which TX appeared) as an approximation because the next miner usually begins the mining process as soon as they receive the previous block, to maximize the success rate.

By the above steps, we reduce the proportion of transactions with negative waiting time from 50% (as encountered in [10]) to less than 5%. The remaining negative waiting time may be caused by inaccurate block timestamps (some miners may put a wrong timestamp accidentally or maliciously, although it cannot deviate from real time too much. Otherwise, the block will be ignored by honest nodes [3]) or errors in estimating  $T_{\text{mempool}}^{\text{TX}}$  (see above). Therefore, we set the waiting time of those transactions to 0. We aggregate the waiting time to block-level by taking quartiles in a manner similar to aggregating gas prices. The median waiting time we mention below are block-level statistics, representing the median of all transaction waiting times in a specific block.

#### 4.4 Miners’ Revenue Data

To investigate how EIP-1559 changes miners’ incentives, we collected data about miners’ revenue.

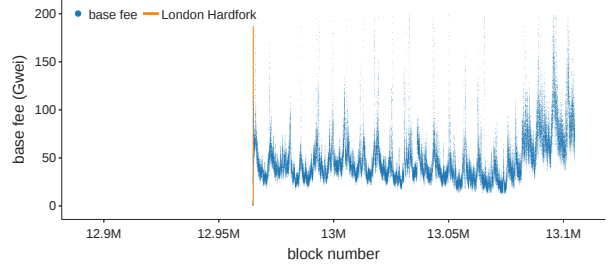
Miners’ revenue (MR) includes block rewards, transaction fees, and “extracted values” (MEV [23]). We can observe the first two components of MR on the blockchain, but it is difficult to completely capture MEV (though previous works, e.g., [63], looked into MEV from specific attacks). We use the revenue from Flashbots, by far the largest MEV extraction services [29], as an approximation of the total MEV.

Flashbots revenue comes in two forms: gas fees of transactions in so-called Flashbots bundles (FBBs) and direct payments to the miners by transactions in FBBs (it is typical for FBB transactions to pay miners by transferring ETH to the coinbase address (the address of the miner who mines the block)). Information about FBB bundles is publicly available [2].

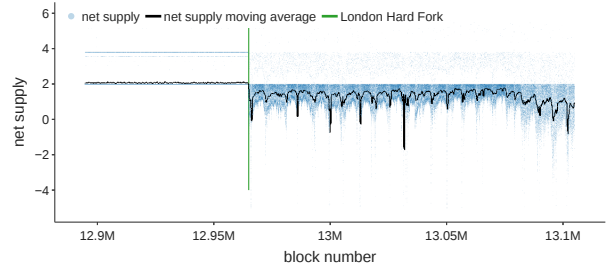
To observe the long-term effect on miners’ revenue (MR), we collected data in a longer window than that in Fig. 1, from block numbers 12,710,000 to 13,510,000 (800,000 blocks in total), i.e., from 40 days before the London Hardfork to 95 days after. Specifically, we divide miner’s revenue into five categories:

- (1) Static block rewards: 2 ETH per block
- (2) Uncle inclusion rewards:  $\frac{1}{32}$  ETH for referencing an uncle block
- (3) Non-FBB gas fees: total gas fees of transactions not in FBBs
- (4) FBB gas fees: total gas fees of transactions in FBBs
- (5) FBB coinbase transfer: total amount of direct payment made by FBBs

As noted above, this division scheme means that we use the revenue from Flashbots as an approximation to MEV, and use all the revenue we can observe as an approximation to miners’ revenue.



(a) Base fee oscillated after London Hardfork with occasional peaks. Each dot represents a block.



(b) Net supply of ETH dropped after London Hardfork, sometimes to negative. Net supply is the number of ETH issued to miners minus that burned as base fees. Each dot represents a block.

**Figure 2: Time Series of Base Fee and ETH net supply**

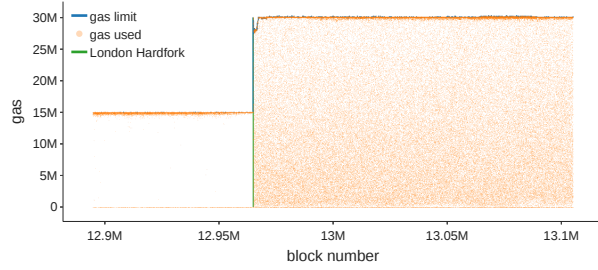
#### 4.5 Fork Rate Data

To understand how the new transaction fee mechanism may affect consensus security, we collected data about past forks in Ethereum. The Ethereum blockchain contains pointers to uncle blocks, from which we derive the number of “siblings” to show the specific time when forks happen. Specifically, a sibling of a block at height  $h$  refers to the uncle blocks (of a later block) with height  $h$ . Sibling count can reflect how many different blocks compete at a specific height at a given time.

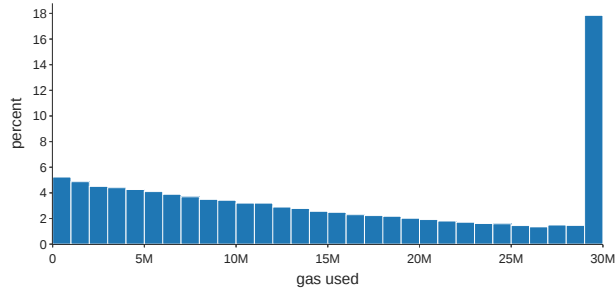
#### 4.6 Preliminary Visualizations

We first visualize some parameters related to EIP-1559 here.

**Base fee dynamics.** Figure 2(a) shows that the base fee oscillated between 30-200 Gwei after the London Hardfork with occasional peaks in high usage periods. With a significant amount of Ether burned as base fee, the issuance rate of Ether reduces significantly. In certain circumstances, blocks could have more Ether burned than minted, resulting in a negative supply of Ether, as shown in Fig. 2(b). Base fee burning can create a positive feedback between Ethereum network activity and Ether price. High demand for Ethereum resources from users drives up both the block gas usage and base fee, which burns more Ether. The reduction of Ether supply induces bullish market sentiment, Ether price appreciation, and ultimately more users. As a result, the reduction of revenue from transaction fees might be partly offset by higher Ether price [39].



(a) Before London Hardfork, almost all blocks used 15 million gas; after London Hardfork, block gas used varies between 0-30 million. Each dot represents a block.



(b) About 20% of blocks after London Hardfork are full (i.e., consume 30M gas).

**Figure 3: Distribution of Block Gas Used**

**Block gas usage.** The new transaction fee mechanism led to rises and falls of base fee as shown above and volatile block gas usage as shown in Fig. 3. In periods of high demand (e.g., NFT airdrop, market crash [57, 74]), block gas used can deviate from its target of 15 million to at most 30 million (or slightly above), in which case the base fee in the next block will increase by at most 12.5% as implied by Eq. (1). Given the current block time of around 13 seconds, the base fee will double every 80 seconds if a series of full blocks are produced. The surge of base fee ensures the limited block space is allocated to transactions with higher intrinsic values. Increasing base fee screens users with lower intrinsic values and leads to fewer transactions included in a block until the block gas used is lower than the target.

**Adoption rate.** Figure 4 shows that the adoption rate of the new transaction fee mechanism has been steadily increasing. Transactions that adopt the EIP-1559 bidding style with max fee and max priority fee is defined to be type-2 (TxnType = 2), while those that stick to the legacy bidding style is defined to be type-0 or type-1 (TxnType = 0 or 1), depending on which points on the elliptic curve are used. We notice a sharp increase in adoption rate around block number 13.05 million, which is possibly related to the adoption as default on MetaMask [6].

## 5 EMPIRICAL RESULTS

In this section, we first present an overview of our methodology in Section 5.1, then we present empirical results to answer the following questions:

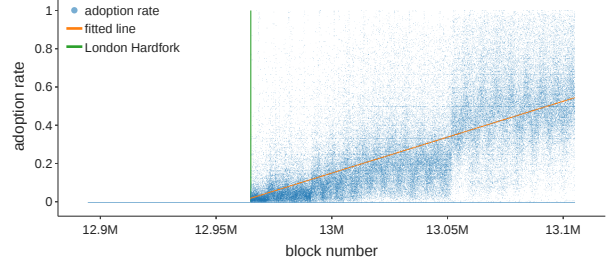


**Figure 4: Adoption of EIP-1559 style bidding steadily increased after London Hardfork. Each dot represents a block.**

- Does EIP-1559 affect the transaction fee dynamics in terms of overall fee level, users’ bidding strategies, and intra-block distribution of fees? (Section 5.2)
- Does EIP-1559 affect the distribution of transaction waiting time? (Section 5.3)
- Does EIP-1559 affect consensus security, in terms of fork rates, network loads, and MEV? (Section 5.4)

### 5.1 Methodology

A key challenge in identifying the effect of EIP-1559 on blockchain characteristics is that we must isolate the effect of EIP-1559 from those of confounding factors, such as price volatility, network instability, and time trend. Our approach is to adopt an event study framework [51] and regression discontinuity design (RDD) [9, 43] to identify the impact of EIP-1559 on the dynamics of Ethereum. RDD is a quasi-experimental evaluation widely used in economics, political science, epidemiology, and related disciplines for the causal inference of an event,<sup>6</sup> here EIP-1559. We exploit the gradual adoption of EIP-1559 several weeks after London Hardfork to set up the RDD framework, using the event of London Hardfork and EIP-1559 adoption rate in each block as the independent variables and estimating both immediate effects of London Hardfork and average treatment effects of EIP-1559 adoption.

We specify the RDD by Eq. (2):

$$Y = \alpha_0 + \alpha_1 \mathbb{1}(\text{London Hardfork}) + \alpha_2 r_{\text{EIP}} + \alpha_3 X + \mu_h + \epsilon. \quad (2)$$

Here,  $\alpha_1$  is the coefficient for the indicator variable on whether London Hardfork happened (block number  $\geq 12965000$ ). It represents the immediate effect of EIP-1559 on the outcome variable  $Y$ .  $\alpha_2$  is the coefficient for  $r_{\text{EIP}}$  the percentage of transactions that adopts EIP-1559 after the London Hardfork. Since EIP-1559 is backward compatible, many users still adopted the legacy bidding style in the few weeks after the upgrade, but the adoption rate kept rising as we show in Fig. 4. By Nov. 2021, 40% to 60% of all transactions [39] use the new bid style. Therefore,  $\alpha_2$  represents the effect of an increase in EIP-1559 adoption.

We include a set of control variables [13] represented as  $X$  in Eq. (2). We control the block number in our sample to account

<sup>6</sup>We refer the readers to Pages 5-8 in Athey and Imbens [9] for more details on regression discontinuity design.

for a possible time trend before the London Hardfork, defined by

$$\text{nblock} = \begin{cases} \text{BlockNumber} - 12895000 & \text{pre-EIP period} \\ \text{BlockNumber} - 12965000 & \text{post-EIP period} \end{cases}$$

We also control the price volatility, median gas price, and return on investment (ROI) (minute-level percentage change in ETH price) to account for the variance in demand for transactions on the Ethereum network. Block size is controlled for network stability. We include an hour fixed-effect term  $\mu_h$  to account for the seasonality of Ethereum network conditions as we can clearly see in Fig. 2(a).  $\epsilon$  is an error term.

## 5.2 Transaction Fee Dynamics

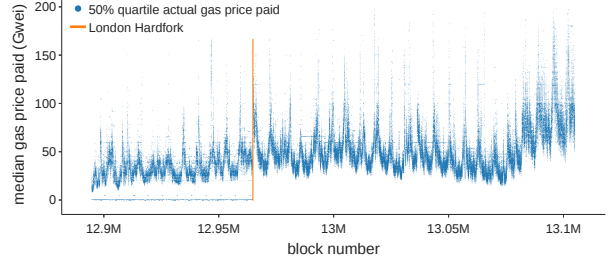
**5.2.1 Overview.** Transaction fee mechanism design is not intended to solve blockchain scalability. Thus, the fee level before and after the London Hardfork did not change substantially. However, it did change how users bid and users' bidding strategy largely coincides with the predictions made by Roughgarden (2020) [68].

Figure 5(a) shows the time series for the actual gas price paid quartiles in each block before and after London Hardfork. With an hourly seasonality (intra-day oscillation due to difference in demand across time zones), the gas price level did not change much before and immediately after the London Hardfork. It is unclear whether the increase in gas price after block number 13.07M is caused by EIP-1559 or other factors.

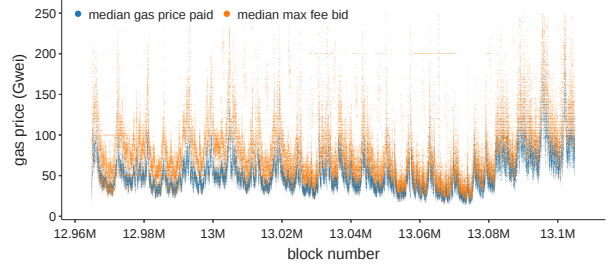
Figure 5(b) and Fig. 5(c) further decompose different fee parameters in users' bids. Figure 5(b) shows that while the median gas price paid and median max fee bid are volatile and highly correlated to each other, the max fee bids are usually higher than the gas prices paid. Meanwhile, Fig. 5(c) shows that the median max priority bid remains at a low level (almost always  $< 10$  Gwei) throughout the period and  $< 3$  Gwei after block number 13.06M). Overall, these results are consistent with the predictions in [68] that the obvious optimal bid is a max fee that represents the intrinsic value of the transaction and a max priority fee that represents the marginal cost of miners' inclusion of the transaction. If these predictions hold, then we would observe max fee bids higher than the actual price paid and a low, stable level of priority fees bid, which is exactly what we observed. Ferreira et al. [28] expressed concerns that the EIP-1559 TFM may degrade to a first-price auction on priority fee when the base fee is set too low. However, our empirical results show that this did not happen much in practice.

Moreover, we also compare the median prices for different transaction types. As shown in Fig. 6, the median gas price paid of the EIP-1559 transactions in a block has a distribution to the left of that of the legacy transactions. The median of median gas price of EIP-1559 transactions in each block is 45 Gwei, while that of legacy transactions is 54 Gwei. This means that users who adopt EIP-1559 bidding overall pays less than those who stick to legacy bidding.

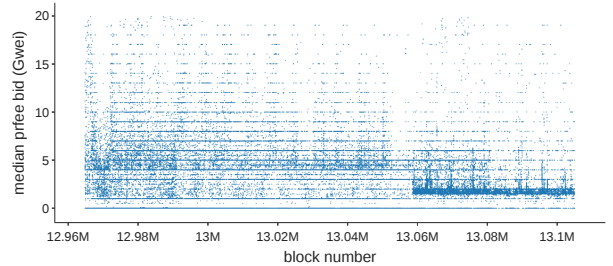
These findings point to the insight that users' fee estimation was made easier by EIP-1559. Before EIP-1559, users must pay the entirety of the bid if their transactions were included, so they risked overpaying gas fees if the network was not as congested as they expected. Due to this concern, users must carefully estimate gas prices and might tend to bid conservatively, as a result of first-price auction [55]. EIP-1559, however, allows users to set two parameters



(a) The gas price paid by users did not change much immediately after London Hardfork, but it started to rise about two weeks later. We can not conclude whether this was caused by EIP-1559. Each dot represents a quartile of the gas price paid for a block.



(b) Max fee bids were usually much higher than the actual gas prices paid. Each dot represents a block.



(c) Priority fee bids remained at low level in most cases ( $< 10$  Gwei), especially after block number 13.06M. Each dot represents a block.

**Figure 5: Overview of Fee Dynamics**

in a bid: a priority fee and a max fee (both for per gas unit). Users only pay the smaller of 1) the sum of the base fee and priority fee bid and 2) the max fee. Therefore, if the network conditions turned out better than expected, the user will only pay the base fee plus the priority fee. This leads to a simple but optimal bidding strategy as shown in [68]. Therefore, EIP-1559 makes fee estimation easier.

**5.2.2 Intra-block inter-quartile range.** If users bid in the obvious optimal bid introduced above, the eventual gas price paid by users who adopt the EIP-1559 style bid would be the base fee plus a small amount of priority fee, so users who adopt the EIP-1559 style bid tend to pay a similar gas price. A direct implication of this is that the intra-block variance of gas prices should significantly

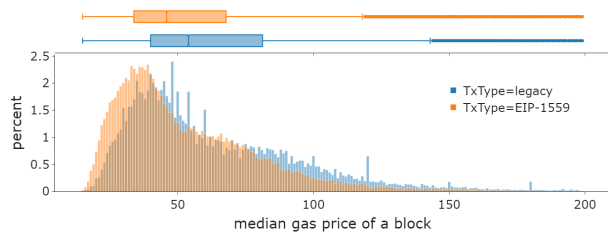
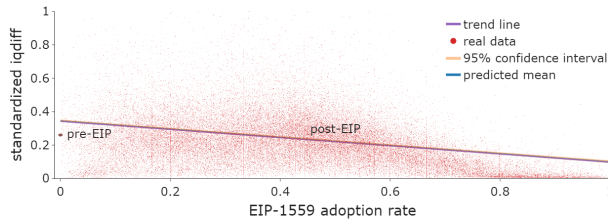


**Figure 6: Distributions of median gas prices of a block for legacy transactions and EIP-1559 transactions. The distribution of EIP-1559 transactions is overall to the left of that of legacy transactions, which means that users who adopt EIP-1559 pay a lower gas price.**



The figure visualizes Column (4) in Table 8. The line in the figure shows the predicted standardized IQR at different levels of EIP-1559 adoption rate based on the linear regression outcome controlling all other factors at a representative scenario (e.g., median gas price at 39 Gwei, price volatility at 0.005). As adoption rate grows from 0 to 1, the predicted mean of standardized inter-quartile difference gradually decreases from 0.34 to 0.09. Before London Hardfork, the average is about 0.27, shown as the red dot on the left side. The scatters are real data. The figure also includes another trend line that displays simple linear regression without controlling any factors, though it largely coincides with the predicted line.

**Figure 7: Simulated relationship between standardized inter-quartile difference and EIP-1559 adoption**

reduce after London Hardfork, especially as more users adopt type-2 transactions. While we cannot directly ease of fee estimation, we manage to measure the intra-block variance of gas prices by standardized inter-quartile range (IQR) (defined in Section 4.2).

The relationship between standardized IQR, London Hardfork, and EIP-1559 is visualized in Fig. 7, which simulates standardized IQR at different levels of EIP-1559 adoption rates based on Column (4) in Table 8. Immediately after the London Hardfork, standardized IQR increases by about 8 percentage points (from 0.26 to 0.34), but as more people adopt the new bidding style, the standardized IQR is predicted to decrease by 24 percentage points (from 0.34 to 0.10) when all users adopt the new bidding style.

Given the scale of this estimate, EIP-1559 should have a large negative effect on the intra-block difference of gas price paid as more users adopt the new bidding style (up to Nov. 2021, the EIP-1559 adoption rate is about 40%-60% [39]). This implies that the inequality of intra-block gas prices decreases, especially as more users adopt EIP-1559 transactions. Thus, we show that the concerns raised by Reijdsbergen et al. [64] relating to the volatility of base fee making fee estimation more difficult does not hold in practice.

### 5.3 Waiting Time

Waiting time is widely modeled in literature as an essential component of users’ utility function, and a short waiting time is crucial to user experience. As a result of easier fee estimation (see above in Section 5.2), a rational user can simply bid their intrinsic value of the transaction without risking overpaying. Thus, with the EIP-1559 upgrade, it should be more straightforward for users to include their transactions in the next available block. We find that waiting time significantly reduces after London Hardfork. This benefits both EIP-1559 and legacy transactions.

The reduction of waiting time can be observed in Fig. 8, which demonstrates the distribution of block median waiting time before and after London Hardfork. Each observation represents a block and the median of transaction waiting times in that block. The distribution shifts leftward after the London Hardfork. The 25th quartile of median block waiting time decreased from 10.7 seconds to 5.5 seconds, the 50th quartile decreased from 16.9 seconds to 10.4 seconds, and the 75th quartile decreased from 34.0 seconds to 18.6 seconds. Moreover, we observe that the waiting time of transactions in both types (legacy or EIP-1559 bidding styles) decreased. The 50th quartile of median legacy-style transaction waiting time across blocks is 9.4 seconds after London Hardfork, while that of median EIP-1559-style transactions waiting time across blocks is 8.9 seconds.<sup>7</sup> This implies that the effect of EIP-1559 adoption spills over even to the transactions that have not adopted the new bidding style by improving the overall gas bid structure in the mempool.

Table 2 further manifests this finding. Column (1)-(3) display regression results with block median waiting time as the dependent variable, the indicator of London Hardfork and EIP-1559 adoption rate as independent variables. The first row in Columns (1) - (3) return consistent and significant negative effects of London Hardfork on waiting time, while the second row in Columns (1) - (3) return consistent and significant negative effects of EIP-1559 adoption on waiting time. We observe that London Hardfork itself has a significant negative effect on the median waiting time of all transactions in blocks, and this effect strengthens over time. Specifically, waiting time decreased on average by about 9 seconds after London Hardfork, and assuming linear treatment effect waiting time would further decrease by another 6-11 seconds when all users adopt EIP-1559 style bidding. The relationship between block median waiting time, London Hardfork, and EIP-1559 adoption rate is visualized in Fig. 9, which simulates waiting time at different levels of EIP-1559 adoption rates based on Column (3) in Table 2.

Columns (4) and (5) in Table 2 display regression results with block median waiting time of only the legacy transactions as the dependent variable, the indicator of London Hardfork and EIP-1559 adoption rate as independent variables. Similarly, the results show that London Hardfork had a consistently and significantly negative effect on median waiting time for legacy transactions. So did the EIP-1559 adoption rate (second row in Columns (4) and (5)). However, the coefficient of these two regressions might be biased by the

<sup>7</sup>Readers may notice that both median legacy-style transaction waiting time and median EIP-1559-style transactions waiting time are shorter than median all transaction waiting time after London Hardfork. This does not contradict the fact that in each block, the median waiting time of all transactions is always between the median waiting time of legacy transactions and the median waiting time of EIP-1559 transactions. The distributions of these three variables are shown in Appendix D Fig. 17

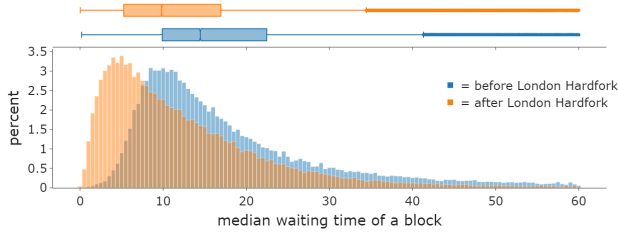
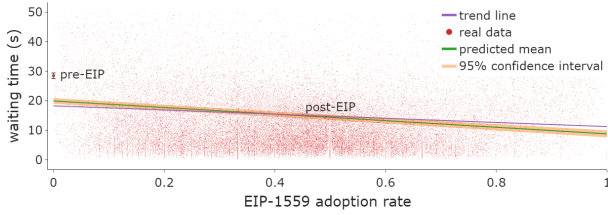


**Figure 8: Distributions of median waiting time. It moved left after the London Hardfork. Users experience a much lower transaction waiting time with EIP-1559.**



The figure visualizes Column (3) in Table 2. The line in the figure shows the predicted block median waiting time at different levels of EIP-1559 adoption rate based on the linear regression outcome controlling all other factors at a representative scenario (e.g., median gas price at 39 Gwei, price volatility at 0.005). As adoption rate grows from 0 to 1, the predicted mean of waiting time gradually decreases from 19.93 seconds to 8.79 seconds. Before London Hardfork, the average is about 28.5 seconds, shown as the red dot on the left side. The scatters are real data. The figure also includes another trend line that displays simple linear regression without controlling any factors.

**Figure 9: Simulated relationship between waiting time and EIP-1559 adoption**

selection of the adoption of EIP-1559. The early adopters of EIP-1559 are likely to be the more sophisticated ones like mining pools and institutional investors. Nonetheless, the spillover effect of EIP-1559 adoption to legacy transactions is convincing given the descriptive statistics mentioned above. Additionally, the significantly positive coefficient on 90-block volatility in Column (3) implies that waiting time is longer when Ether price volatility is higher.

### 5.4 Consensus Security

The Ethereum community has discussed extensively the security implications of EIP-1559 [16, 17], and the community largely agreed that it should not compromise consensus security. We investigate three avenues here through which EIP-1559 might affect consensus: fork rates, network load, and Miner Extractable Value (MEV). With existing evidence, we tend to believe that EIP-1559 does not make the Ethereum system substantially more insecure.

**5.4.1 Fork rates.** Fork rate is an important indicator for consensus security. Prevalence of forks (or so called “uncle blocks” in Ethereum) can lead to higher vulnerability to double-spend attacks and selfish mining [32]. EIP-1559 changes the distribution of block sizes, so we would like to understand its implication on fork rates. We use the terms “uncle rates” and “fork rates” interchangeably.

	median waiting time				
	(1) All Tx	(2) All Tx	(3) All Tx	(4) Legacy Tx	(5) Legacy Tx
London Hardfork	-9.321*** (0.396)	-9.690*** (0.396)	-8.544*** (0.394)	-4.377*** (0.405)	-3.672*** (0.404)
EIP-1559 adoption	-6.140*** (0.583)	-5.956*** (0.583)	-11.147*** (0.585)	-21.889*** (0.597)	-26.560*** (0.601)
nblock	-0.000*** (0.000)	-0.000*** (0.000)	-0.000*** (0.000)	-0.000*** (0.000)	-0.000*** (0.000)
median gas price		-0.005*** (0.001)	0.000 (0.001)		-0.002 (0.001)
90-block volatility		-117.532*** (9.332)	140.746*** (46.046)		133.191*** (47.268)
size			0.000*** (0.000)		0.000*** (0.000)
ROI			-232.497*** (46.677)		-217.323*** (47.915)
Intercept	28.062*** (0.191)	24.300*** (0.381)	15.069*** (0.494)	28.281*** (0.196)	16.363*** (0.507)
Observations	138,043	137,795	137,794	138,043	137,794
R <sup>2</sup>	0.736	0.737	0.744	0.728	0.734

Note: Hour fixed effect included. \*p<0.1; \*\*p<0.05; \*\*\*p<0.01

Linear regression with block median waiting time as dependent variable, indicator of London Hardfork and EIP-1559 adoption rate as independent variables with different sets of controls shown in different columns. Outcome variable data trimmed to <300s to avoid extreme outliers (4% of data). Standard errors are in parentheses. Median waiting time dropped significantly after London Hardfork. It further drops in the blocks with higher adoption rate of EIP-1559 style bidding. The data frequency is by block. Column (3) of this table is visualized in Fig. 9.

**Instructions for reading the tables:** 1) the table header shows the dependent variable. (i.e., all transactions and legacy transactions median waiting time in each block); 2) the index column presents the independent variables. (i.e., London Hardfork, EIP-1559 adoption, nblock, etc.); 3) each column labelled with number presents result of one regression in the form of Eq. (2) as introduced in Section 5.1; 4) each number presents the effect of the independent variable (the row index) on the dependent variable after controlling for other independent variables (if in the same column, the output of that row is not blank); For example, in Column (1), -9.321 presents the effect of London Hardfork on all transaction median waiting time; 5) when the number is positive (negative), the dependent variable increases (decreases) on average by the absolute value of the number as the independent variable increases by 1 unit; For example, in Column (1), -9.321 means when London Hardfork turns from 0 to 1 (when it happens), transaction waiting time decreases by 9.321 on average; 6) the stars show the significance level of a t-test, i.e., the error rate to reject the null hypothesis that the independent variable has no effect on the dependent variable; For example, in Column (2), there are three stars for the row with index “EIP-1559 adoption”, which means that if the null hypothesis is true (EIP-1559 adoption has no effect on waiting time), there is only 1% chance we will see data as extreme as this; 8) If a cell is left blank, the variable is not included in the regression presented by the column. With different cells left blank, we present regression results with different variables included. These instructions also guide the reading of Table 3 and Table 8.

**Table 2: Waiting Time and EIP-1559 Adoption**

We investigate the relationship between EIP-1559, block gas used, block size, and the number of uncles in this section and conclude that the influence of EIP-1559 on the number of uncle blocks is marginal. We also find that EIP-1559 increased block size on average, which led to a higher fork rate.

Column (1) of Table 3 shows results of a linear regression between block size and London Hardfork. It indicates that the average size increased from 64.05 kbytes (intercept in Column (1)) before London Hardfork to 78.01 kbytes (adding the intercept with the

coefficient on London Hardfork) after London Hardfork by 13.96 kbytes (London Hardfork coefficient in Column (1)). Still using block size as the dependent variable and London Hardfork as the independent variable, Column (2) further controls EIP-1559 adoption rate, gas used, and the interaction term between London Hardfork and gas used. The results show that London Hardfork itself, adoption rate, and gas used are all positively and significantly associated to block size. With these two columns, we conclude that block size increases significantly after London Hardfork and grows with EIP-1559 adoption.

Column (3) of Table 3 shows the result of logistic regression with the indicator of whether a block has siblings as the dependent variable and block size in kbytes as the independent variable. The result shows that as block size grows bigger, the likelihood that a block has siblings becomes significantly larger. (The coefficient of block size in Columns (3), 0.0034, is positive and with three stars.) Together with Columns (1) and (2), our results suggest that EIP-1559 could also increase the likelihood of sibling appearance by increasing block size.

Column (4) further controls the event of London Hardfork and EIP-1559 adoption, which suggests alternative mechanisms on how EIP-1559 might affect sibling appearance. After controlling for block size, EIP-1559 still had a weak positive effect (the coefficient of London Hardfork, 0.0704, is positive with one star, i.e. a larger p-value) on sibling appearance, but EIP-1559 adoption (the coefficient on EIP-1559 adoption, -0.2257, is negative with three stars) has a significantly negative effect. These estimates present evidence that EIP-1559 affects sibling appearance mainly through block size with other unknown channels for further research.

**5.4.2 Network load.** A debated point about the security implications of EIP-1559 is whether it will put the system under a higher load [16, 17]—i.e., whether it will require nodes to perform more computational, networking, and storage work to participate in the blockchain protocol—due to increased block size cap (from 15M to 30M) and skewed distribution of block gas used (see Fig. 3).

The blog post Buterin (2021) [17] mentions that “block variance is nothing to worry about”. One of the arguments in favor is that short-term spikes happen already before the London Hardfork—due to the Poisson process inherent to proof of work mining. This being true, it is unclear how the pre-London-Hardfork spikes compare to the post-London-Hardfork ones, as EIP-1559 introduces bigger blocks that might contribute to more frequent and intense spikes (the stochastic nature of block production would have the same effect before and after London Hardfork).

We define the average load of the Ethereum system in a given period  $T$  as the average of gas consumed per second in  $T$ . We calculated the average load for varying time intervals (20-120 seconds) at each block timestamp and compared the distributions before and after London Hardfork. The results are shown in Fig. 10. We also select various thresholds to define the load spike and calculate the percentage of load spikes before and after London Hardfork, as shown in Table 4. From Fig. 10 and Table 4, we can find that EIP-1559 does not affect integral network load and frequency of load spikes to a significant degree, especially not for an extended period (e.g., 40 seconds or 3 blocks or more). Our results confirm the argument from Buterin’s blog post [17].

	block size	
	(1)	(2)
London Hardfork	13960.686*** (225.731)	25126.760*** (7494.917)
EIP-1559 adoption		25803.954*** (357.959)
gas used		0.006*** (0.001)
London Hardfork * gas used		-0.002*** (0.001)
Intercept	64051.066*** (159.455)	-33113.125*** (7492.033)
Observations	138,055	138,055
R <sup>2</sup>	0.027	0.726

Standard errors in parentheses. Column (1) and (2) show the linear regression with block size (in bytes) as dependent variable and London Hardfork and EIP-1559 adoption as independent variables. Block size became larger on average after London Hardfork, and it was larger when the block had high EIP-1559 adoption rate or high gas usage. The data frequency is by block.

	sibling indicator	
	(3)	(4)
block size (kbyte)	0.0034*** (0.0003)	0.0036*** (0.0003)
London Hardfork		0.0704* (0.0400)
EIP-1559 adoption		-0.2257*** (0.0764)
Intercept	-3.2573*** (0.0249)	-3.2608*** (0.0263)
Observations	138,055	138,055
Logistic regression used; *p<0.1; **p<0.05; ***p<0.01		

Standard errors in parentheses. Column (3) and (4) show the linear regression with block size (in bytes) as dependent variable and London Hardfork and EIP-1559 adoption as independent variables. Block size became larger on average after London Hardfork, and it was larger when the block had high EIP-1559 adoption rate or high gas usage. The data frequency is by block.

**Table 3: Sibling existence, block size, and EIP-1559**

**5.4.3 Miner Extractable Value (MEV).** MEV refers to the profit a miner can make through their ability to arbitrarily include, exclude, or re-order transactions within the blocks they produce. As [23] pointed out, significant MEV can incentivize miners to deviate from the consensus protocol (e.g., to fork, or even rewind the blockchain to collect the profit in MEV [23]). The volume and change of MEV have a profound impact on consensus.

We focus on the MEV data we described in Section 4.4 to observe the impact of EIP-1559 on miners’ revenue. We notice that the miners’ revenue from MEV dropped temporarily after the London fork, though soon recovered to the level before. However, in the end, miners’ revenue from MEV became a much larger share of miners’ revenue. This might create an incentive for miners to invest more in MEV extraction.

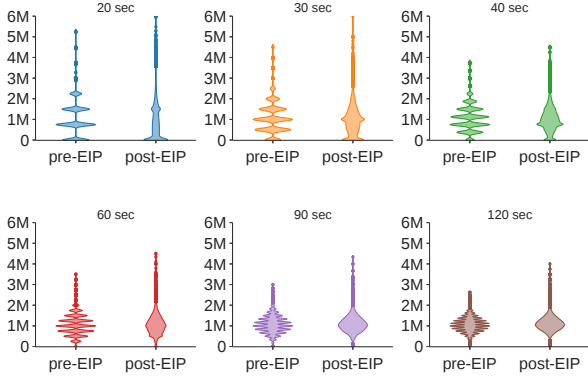


**Figure 10: Moving averages of block gas used per second for different time intervals**

Pre London Hardfork									
period\threshold	1.0 M	1.2 M	1.4 M	1.6 M	1.8 M	2.0 M	2.2 M	2.4 M	
20 s	39.99	39.98	39.97	14.64	14.64	14.64	14.59	3.90	
30 s	35.29	34.40	34.39	14.67	14.66	5.07	4.92	4.92	
40 s	53.98	30.33	30.32	13.97	13.96	5.39	5.38	1.78	
60 s	42.22	41.90	24.26	12.37	5.57	2.26	2.23	0.83	
90 s	46.22	30.56	18.37	10.17	5.16	1.05	0.40	0.16	
120 s	49.20	35.10	14.41	8.25	2.30	0.52	0.24	0.03	
Post London Hardfork									
period\threshold	1.0 M	1.2 M	1.4 M	1.6 M	1.8 M	2.0 M	2.2 M	2.4 M	
20 s	39.11	31.88	25.66	15.12	10.38	7.27	5.00	3.38	
30 s	42.85	29.43	20.41	13.46	8.60	5.01	2.73	1.55	
40 s	45.57	31.45	20.46	11.41	6.35	3.35	1.76	0.86	
60 s	52.28	32.70	18.23	8.90	4.09	1.76	0.74	0.32	
90 s	57.77	33.83	16.27	6.54	2.35	0.80	0.30	0.13	
120 s	61.75	34.23	14.71	5.04	1.56	0.45	0.17	0.05	

**Table 4: Percentage of network spikes for different time intervals and different thresholds**

*Miners’ revenue before and after EIP-1559.* Figure 11(a) shows the miners’ total revenue and its composition. Overall, miners’ revenue decreased after the EIP, primarily because the base fees are burned.

Figure 11(b) plots the revenue from MEV. After a downturn for less than 50,000 blocks, MEV revenue quickly recovers to the level before London Hardfork. This may have been caused by the following reasons: 1) Flashbots searchers needing to update their software after London Hardfork in order to adapt to EIP-1559, and 2) potentially having high volatility of miner extractable value due to network instability in the short term after London Hardfork.

Figure 11(c) and Fig. 11(d) show the ratio of MEV revenue to the total revenue and to the non-static revenue (i.e., miners’ revenue minus the static block reward), respectively. As the revenue from gas fees dropped dramatically post London Hardfork while MEV revenue recovered quickly, the ratio between MEV and total revenue increased significantly, as shown in Fig. 11(c) and Fig. 11(d), after London Hardfork, miners’ MEV revenue accounts for about 4% of the total revenue and about 30% of the

non-static revenue, while before London Hardfork, the MEV revenue is only about 3% of the total revenue and about 15% of the non-static revenue.

*Distribution of non-static revenue before and after EIP-1559.* Miners’ non-static revenue consists of three parts: uncle inclusion rewards, revenue from Flashbots bundles (i.e., “FBB gas fee” plus “FBB coinbase transfer”) and non-FBB gas fee. The uncle inclusion reward is typically small and can be ignored.

As Fig. 12 shows, the distribution of non-static revenue changed significantly after EIP-1559. Figure 12(b) and Fig. 12(c) further break the changes down. Figure 12(b) shows the distribution of revenue from Flashbots bundles, which does not change much before and after London Hardfork. Figure 12(c) shows the distribution of “non-FBB gas fee”. This part of the revenue is very different before and after London Hardfork and is the main reason for the change in the distribution of miners’ revenue.

From Fig. 12, we conclude EIP-1559 does not change the distribution of MEV revenue in the short term, but it significantly changes that of non-FBB gas fees.

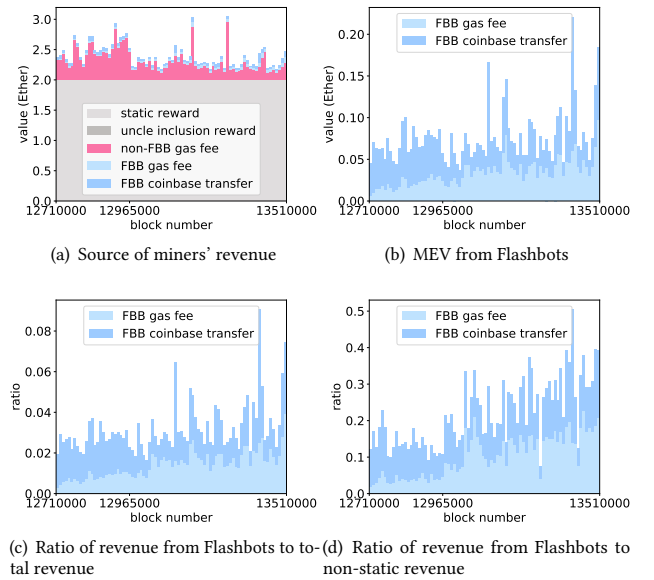


**Figure 11: Sources and changes of miners’ revenue**

## 6 CONCLUSION

We evidence how a major TFM reform on Ethereum affects the blockchain dynamics of Ethereum. Our empirical study relates to and tests implications for a wide range of existing theoretical research. For instance, our results on users’ bids are consistent with the predictions in Roughgarden (2020) [68] that the obvious optimal bid under EIP-1559 is a max fee that represents the intrinsic value of the transaction and a max priority fee that represents the marginal cost of miners’ inclusion of the transaction. Ferreira et al. [28] concern that the EIP-1559 TFM may degrade to a first-price auction on the priority fee when the base fee is too low. Their concern is

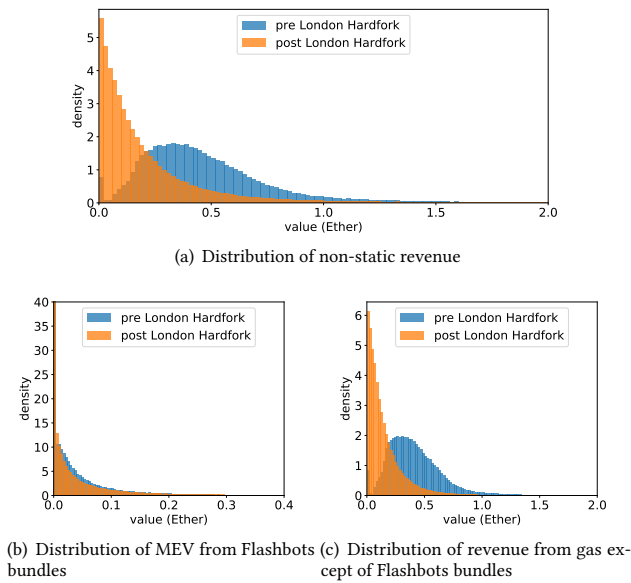


**Figure 12: Distribution of non-static revenue before and after London Hardfork**

valid, but our empirical results show that this rarely happened in reality. Reijsbergen et al. [64] concern that the volatility of base fees after EIP-1559 would make it more difficult for users to estimate transaction fees. In comparison, we show that the volatility of intra-block gas prices decreases significantly as more users adopt EIP-1559 transactions, which implies easier fee estimation and better user experience. We also improve the measurement strategy of transaction waiting time in previous studies, largely eliminating the influence of negative waiting time encountered by Azevedo-Sousa et al. [10].

We present several new findings that are absent from existing theoretical research. First, our result shows that EIP-1559 increases user experience by reducing waiting time significantly. However, its mechanism remains largely unknown and is not yet modeled in existing literature. Second, we found that when Ether’s price is more volatile, the transaction fee and waiting time are significantly higher, suggesting that price volatility can be one policy parameter for the future design of TFM. Finally, we also verify that a larger block size increases the presence of siblings. Even though the effect size through EIP-1559 is negligible, we shall consider this for future updates, for instance, when further enlarging the block gas limit.

**REFERENCES**

[1] [n. d.]. *ethereum/go-ethereum: Official Go implementation of the Ethereum protocol*. <https://github.com/ethereum/go-ethereum>

[2] [n. d.]. *Flashbots Dashboards*. <https://dashboard.flashbots.net/>

[3] [n. d.]. *Max seconds from current time allowed for blocks, before they're considered future blocks*. <https://github.com/ethereum/go-ethereum/blob/master/consensus/ethash/consensus.go#L46>

[4] [n. d.]. *Send private transactions by TaiChi on Ethereum*. [https://github.com/Taichi-Network/docs/blob/master/sendPrivateTx\\_tutorial.md](https://github.com/Taichi-Network/docs/blob/master/sendPrivateTx_tutorial.md)

[5] 2021. *Eden Network*. <https://www.edennetwork.io/>

[6] 2021. *MetaMask 1559*. <https://metamask.io/1559#1559-video>

[7] Guillermo Angeris, Hsien-Tang Kao, Rei Chiang, Charlie Noyes, and Tarun Chitra. 2019. *An analysis of Uniswap markets*. <https://arxiv.org/abs/1911.03380>

[8] Lennart Ante. 2021. *Smart contracts on the blockchain – A bibliometric analysis and review*. *Telematics and Informatics* 57 (03 2021), 101519. <https://doi.org/10.1016/j.tele.2020.101519>

[9] Susan Athey and Guido W. Imbens. 2017. *The State of Applied Econometrics: Causality and Policy Evaluation*. *Journal of Economic Perspectives* 31 (05 2017), 3–32. <https://doi.org/10.1257/jep.31.2.3>

[10] José Eduardo Azevedo Sousa, Vinicius Oliveira, Júlia Valadares, Glauber Dias Gonçalves, Saulo Moraes Villela, Heder Soares Bernardino, and Alex Borges Vieira. 2020. *An analysis of the fees and pending time correlation in Ethereum*. *International Journal of Network Management* 31 (07 2020). <https://doi.org/10.1002/nem.2113>

[11] Massimo Bartoletti, James Hsin-yu Chiang, and Alberto Lluch Lafuente. 2021. *SoK: Lending Pools in Decentralized Finance*. *FC 2021: Financial Cryptography and Data Security* (2021), 553–578. [https://doi.org/10.1007/978-3-662-63958-0\\_40](https://doi.org/10.1007/978-3-662-63958-0_40)

[12] Soumya Basu, David Easley, Maureen O’Hara, and Emin Siler. 2021. *StableFees: A Predictable Fee Market for Cryptocurrencies*. *SSRN Electronic Journal* (07 2021). <https://doi.org/10.2139/ssrn.3318327>

[13] MATTHEW BLACKWELL and ADAM N. GLYNN. 2018. *How to Make Causal Inferences with Time-Series Cross-Sectional Data under Selection on Observables*. *American Political Science Review* 112 (08 2018), 1067–1082. <https://doi.org/10.1017/s0003055418000357>

[14] Vitalik Buterin. 2013. *Ethereum Whitepaper*. <https://ethereum.org/en/whitepaper/>

[15] Vitalik Buterin. 2018. *Blockchain Resource Pricing*. <https://ethresear.ch/t/draft-position-paper-on-resource-pricing/2838>

[16] Vitalik Buterin. 2021. *EIP 1559 FAQ*. <https://notes.ethereum.org/@vbuterin/eip-1559-faq#Might-EIP-1559-run-the-risk-of-over-stressing-nodes-and-miners-during-periods-of-high-usage>

[17] Vitalik Buterin. 2021. *Why I think EIP 1559 block variance is nothing to worry about*. [https://notes.ethereum.org/@vbuterin/eip\\_1559\\_spikes](https://notes.ethereum.org/@vbuterin/eip_1559_spikes)

[18] Miles Carlsten, Harry Kalodner, S. Matthew Weinberg, and Arvind Narayanan. 2016. *On the Instability of Bitcoin Without the Block Reward*. *Proceedings of the 2016 ACM SIGSAC Conference on Computer and Communications Security - CCS’16* (2016). <https://doi.org/10.1145/2976749.2978408>

[19] Huashan Chen, Marcus Pendleton, Laurent Njilla, and Shouhuai Xu. 2020. *A Survey on Ethereum Systems Security*. *Comput. Surveys* 53 (07 2020), 1–43. <https://doi.org/10.1145/3391195>

[20] Tarun Chitra. 2020. *Competitive Equilibria Between Staking and On-chain Lending*. *Cryptoeconomic Systems* (11 2020). <https://doi.org/10.21428/58320208.9ce1cd26>

[21] Kyle Croman, Christian Decker, Ittay Eyal, Adem Efe Gencer, Ari Juels, Ahmed Kosba, Andrew Miller, Prateek Saxena, Elaine Shi, Emin Gün Siler, Dawn Song, and Roger Wattenhofer. 2016. *On Scaling Decentralized Blockchains*. *Financial Cryptography and Data Security* (2016), 106–125. [https://doi.org/10.1007/978-3-662-53357-4\\_8](https://doi.org/10.1007/978-3-662-53357-4_8)

[22] Kyle Croman, Christian Decker, Ittay Eyal, Adem Efe Gencer, Ari Juels, Ahmed Kosba, Andrew Miller, Prateek Saxena, Elaine Shi, Emin Gün Siler, et al. 2016. *On scaling decentralized blockchains*. In *International conference on financial cryptography and data security*. Springer, 106–125.

[23] Philip Daian, Steven Goldfeder, Tyler Kell, Yunqi Li, Xueyuan Zhao, Iddo Bentov, Lorenz Breidenbach, and Ari Juels. 2019. *Flash Boys 2.0: Frontrunning, Transaction Reordering, and Consensus Instability in Decentralized Exchanges*. <https://arxiv.org/abs/1904.05234>

[24] Christian Decker and Roger Wattenhofer. 2013. *Information propagation in the Bitcoin network*. *IEEE P2P 2013 Proceedings* (09 2013). <https://doi.org/10.1109/p2p.2013.6688704>

[25] Nicola Dimitri. 2021. *View of Transaction Fees, Block Size Limit, and Auctions in Bitcoin*. *Ledger Journal* 4 (2021). <http://ledger.pitt.edu/ojs/ledger/article/view/145/153>

[26] David Easley, Maureen O’Hara, and Soumya Basu. 2019. *From mining to markets: The evolution of bitcoin transaction fees*. *Journal of Financial Economics* 134 (10 2019), 91–109. <https://doi.org/10.1016/j.jfineco.2019.03.004>

[27] Ittay Eyal and Emin Gün Siler. 2014. *Majority Is Not Enough: Bitcoin Mining Is Vulnerable*. *Financial Cryptography and Data Security* (2014), 436–454. [https://doi.org/10.1007/978-3-662-45472-5\\_28](https://doi.org/10.1007/978-3-662-45472-5_28)

[28] Matheus Ferreira, Daniel Moroz, David Parkes, and Mitchell Stern. 2021. *Dynamic Posted-Price Mechanisms for the Blockchain Transaction-Fee Market*. <https://arxiv.org/pdf/2103.14144.pdf>

[29] flashbots. 2021. *flashbots/pm: Everything there is to know about Flashbots*. <https://github.com/flashbots/pm>

[30] Ethereum Foundation. 2019. *Ethereum Constantinople/St. Petersburg Upgrade Announcement*. <https://blog.ethereum.org/2019/02/22/ethereum-constantinople-st-petersburg-upgrade-announcement/>

[31] Ethereum Foundation. 2021. *London Mainnet Announcement*. <https://blog.ethereum.org/2021/07/15/london-mainnet-announcement/>

- [32] Arthur Gervais, Ghassan O. Karame, Karl Wüst, Vasileios Glykantzis, Hubert Ritzdorf, and Srđjan Capkun. 2016. On the Security and Performance of Proof of Work Blockchains. *Proceedings of the 2016 ACM SIGSAC Conference on Computer and Communications Security - CCS'16* (2016). <https://doi.org/10.1145/2976749.2978341>
- [33] Lewis Gudgeon, Pedro Moreno-Sanchez, Stefanie Roos, Patrick McCorry, and Arthur Gervais. 2020. SoK: Layer-Two Blockchain Protocols. *Financial Cryptography and Data Security* (2020), 201–226. [https://doi.org/10.1007/978-3-030-51280-4\\_12](https://doi.org/10.1007/978-3-030-51280-4_12)
- [34] Campbell R Harvey, Ashwin Ramachandran, and Joey Santoro. 2021. *Defi And The Future Of Finance*. John Wiley.
- [35] Charles A. Holt and Roger Sherman. 1982. Waiting-Line Auctions. *Journal of Political Economy* 90 (1982), 280–294. <https://www.jstor.org/stable/pdf/1830293.pdf?refreqid=excelsior%3Aaddc7a661c657fba84a5ec04ca1bb70c>
- [36] Nicolas Houy. 2014. The Economics of Bitcoin Transaction Fees. <https://ssrn.com/abstract=2400519>
- [37] Gur Huberman, Jacob D Leshno, and Ciamac Moallemi. 2021. Monopoly without a Monopolist: An Economic Analysis of the Bitcoin Payment System. *Review of Economic Studies* (03 2021). <https://doi.org/10.1093/restud/rdab014>
- [38] Noyan Ilk Ilk, Guangzhi Shang, Shaokun Fan, and J. Leon Zhao. 2021. Stability of Transaction Fees in Bitcoin: A Supply and Demand Perspective. *MIS Quarterly* 45 (06 2021), 563–592. <https://doi.org/10.25300/MISQ/2021/15718>
- [39] Dave Kim. 2021. An Analysis of Ethereum Gas Prices and EIP-1559 Adoption. <https://www.blocknative.com/blog/eip-1559-adoption>
- [40] Piyush Kumar, Manohar U. Kalwani, and Maqbool Dada. 1997. The Impact of Waiting Time Guarantees on Customers' Waiting Experiences. *Marketing Science* 16 (11 1997), 295–314. <https://doi.org/10.1287/mksc.16.4.295>
- [41] Ron Lavi, Or Sattath, and Aviv Zohar. 2019. Redesigning Bitcoin's fee market. *The World Wide Web Conference on - WWW '19* (2019). <https://doi.org/10.1145/3308558.3313454>
- [42] France Leclerc, Bernd H. Schmitt, and Laurette Dube. 1995. Waiting Time and Decision Making: Is Time like Money? *Journal of Consumer Research* 22 (06 1995), 110. <https://doi.org/10.1086/209439>
- [43] David S Lee and Thomas Lemieux. 2010. Regression Discontinuity Designs in Economics. *Journal of Economic Literature* 48 (06 2010), 281–355. <https://doi.org/10.1257/jel.48.2.281>
- [44] Alfred Lehar and Christine A. Parlour. 2020. Miner Collusion and the BitCoin Protocol. *SSRN Electronic Journal* (2020). <https://doi.org/10.2139/ssrn.3559894>
- [45] Stefanos Leonardos, Barnabé Monnot, Daniel Reijbergen, Stratis Skoulakis, and Georgios Piliouras. 2021. Dynamical Analysis of the EIP-1559 Ethereum Fee Market. (06 2021). <https://arxiv.org/pdf/2102.10567.pdf>
- [46] Yoav Lewenberg, Yoram Bachrach, Yonatan Sompolsinsky, Aviv Zohar, and Jeffrey S. Rosenschein. 2015. Bitcoin Mining Pools: A Cooperative Game Theoretic Analysis. *Proceedings of the 2015 International Conference on Autonomous Agents and Multiagent Systems* (05 2015), 919–927. <https://dl.acm.org/doi/10.5555/2772879.2773270>
- [47] Kai Li, Yibo Wang, and Yuzhe Tang. 2021. DETER: Denial of Ethereum Txpool sERvices. In *CCS '21: 2021 ACM SIGSAC Conference on Computer and Communications Security, Virtual Event, Republic of Korea, November 15 - 19, 2021*, Yongdae Kim, Jong Kim, Giovanni Vigna, and Elaine Shi (Eds.). ACM, 1645–1667. <https://doi.org/10.1145/3460120.3485369>
- [48] Shengwu Li. 2017. Obviously Strategy-Proof Mechanisms. *American Economic Review* 107 (11 2017), 3257–3287. <https://doi.org/10.1257/aer.20160425>
- [49] Iuon-Chang Lin and Tzu-Chun Liao. 2017. A Survey of Blockchain Security Issues and Challenges. *International Journal of Network Security* 19 (2017), 653–659. [https://doi.org/10.6633/IJNS.201709.19\(5\).01](https://doi.org/10.6633/IJNS.201709.19(5).01)
- [50] Bloomberg L.P. 2019. XETUSD. [https://bba.bloomberg.net/?utm\\_source=bloomberg-menu&utm\\_medium=terminal](https://bba.bloomberg.net/?utm_source=bloomberg-menu&utm_medium=terminal)
- [51] A. Craig MacKinlay. 1997. Event Studies in Economics and Finance. *Journal of Economic Literature* 35 (1997), 13–39. <https://www.jstor.org/stable/pdf/2729691.pdf?refreqid=excelsior%3A36e33d49e7b7feca7fbf4ea62ab8ca9>
- [52] R. Preston McAfee and John McMillan. 1987. Auctions and Bidding. *Journal of Economic Literature* 25 (1987), 699–738. <https://www.jstor.org/stable/pdf/2726107.pdf?refreqid=excelsior%3A68c5df384014cf64d2c59f3545422e7>
- [53] Satoshi Nakamoto. 2008. Bitcoin: a Peer-to-Peer Electronic Cash System. <https://bitcoin.org/bitcoin.pdf>
- [54] Michael Neuder, Daniel J. Moroz, Rithvik Rao, and David C. Parkes. 2020. Selfish Behavior in the Tezos Proof-of-Stake Protocol. *Cryptoeconomic Systems* (12 2020). <https://doi.org/10.21428/58320208.27350920>
- [55] Dusit Niyato, Nguyen Cong Luong, Ping Wang, and Zhu Han. 2020. Auction Theory for Computer Networks. (05 2020). <https://doi.org/10.1017/9781108691079>
- [56] Fellowship of Ethereum Magicians. 2019. EIP-1559: Fee market change for ETH 1.0 chain. <https://ethereum-magicians.org/t/eip-1559-fee-market-change-for-eth-1-0-chain/2783>
- [57] Best Owie. 2021. Here's The Reason Behind The Spike In Ethereum Gas Fees. <https://bitcoinist.com/heres-the-reason-behind-the-spike-in-ethereum-gas-fees/>
- [58] Emiliano S Pagnotta. 2021. Decentralizing Money: Bitcoin Prices and Blockchain Security. *The Review of Financial Studies* (01 2021). <https://doi.org/10.1093/rfs/hhaa149>
- [59] Rafael Pass and Elaine Shi. 2017. FruitChains. *Proceedings of the ACM Symposium on Principles of Distributed Computing* (07 2017). <https://doi.org/10.1145/3087801.3087809>
- [60] Google Cloud Platform. 2019. Big Query Public Data - crypto\_ethereum. <https://cloud.google.com/bigquery/public-data>
- [61] Proceedings of the 22nd ACM Conference on Economics and Computation (EC). To appear. 2021. *Transaction Fee Mechanism Design*. Proceedings of the 22nd ACM Conference on Economics and Computation (EC). To appear. <https://arxiv.org/abs/2106.01340>
- [62] Ethereum Improvement Proposals. 2021. Ethereum Improvement Proposals. <https://eips.ethereum.org/EIPS/eip-1559>
- [63] Kaihua Qin, Liyi Zhou, and Arthur Gervais. 2021. Quantifying Blockchain Extractable Value: How dark is the forest? <https://arxiv.org/abs/2101.05511>
- [64] Daniël Reijbergen, Shyam Sridhar, Barnabé Monnot, Stefanos Leonardos, Stratis Skoulakis, and Georgios Piliouras. 2021. Transaction Fees on a Honeymoon: Ethereum's EIP-1559 One Month Later. <https://arxiv.org/abs/2110.04753>
- [65] Ling Ren. 2019. Analysis of Nakamoto Consensus. *IACR Cryptol. ePrint Arch.* 2019 (2019), 943.
- [66] Peter Rizun. 2015. A Transaction Fee Market Exists Without a Block Size Limit. <https://www.bitcoinunlimited.info/resources/feemarket.pdf>
- [67] Alvin E. Roth. 2002. The Economist as Engineer: Game Theory, Experimentation, and Computation as Tools for Design Economics. *Econometrica* 70 (07 2002), 1341–1378. <https://doi.org/10.1111/1468-0262.00335>
- [68] Tim Roughgarden. 2020. Transaction Fee Mechanism Design for the Ethereum Blockchain: an Economic Analysis of EIP-1559. <http://timroughgarden.org/papers/eip1559.pdf>
- [69] Konstantin Sokolov. 2021. Ransomware activity and blockchain congestion. *Journal of Financial Economics* 141 (08 2021), 771–782. <https://doi.org/10.1016/j.jfineco.2021.04.015>
- [70] Yonatan Sompolsinsky and Aviv Zohar. 2015. Secure High-Rate Transaction Processing in Bitcoin. , 507–527 pages. [https://doi.org/10.1007/978-3-662-47854-7\\_32](https://doi.org/10.1007/978-3-662-47854-7_32)
- [71] Yonatan Sompolsinsky and Aviv Zohar. 2017. Bitcoin's Underlying Incentives - ACM Queue. <https://queue.acm.org/detail.cfm?id=3168362>
- [72] Kwok Ping Tsang and Zichao Yang. 2021. The market for bitcoin transactions. *Journal of International Financial Markets, Institutions and Money* 71 (03 2021), 101282. <https://doi.org/10.1016/j.intfin.2021.101282>
- [73] Andrew Chi-Chih Yao. 2018. An Incentive Analysis of some Bitcoin Fee Designs. <https://arxiv.org/pdf/1811.02351.pdf>
- [74] Martin Young. 2021. NFT Mania Sends Ethereum Gas Prices to 14 Week High. <https://cryptopotato.com/nft-mania-sends-ethereum-gas-prices-to-14-week-high/>
- [75] Luyao Zhang and Dan Levin. 2017. Bounded Rationality and Robust Mechanism Design: An Axiomatic Approach. *American Economic Review* 107 (5 2017), 235–39. <https://doi.org/10.1257/aer.p20171030>

## A DATA DICTIONARY

We present a full view of the data sets we use and the variables in them in Table 5.

## B STATISTICS TESTS

### Correlation Tests

Figure 13 presents the triangle correlation heatmap between the control variables we use.

### Stationary Tests

Table 6 presents the results of the Augmented Dickey-Fuller (ADF) test for all variables we use. It proves that they are all stationary.

### Auto-correlation Tests

Figure 14 presents the auto-correlation test for the dependent variables we put in the regressions. Gas prices have a significant auto-correlation, while the autocorrelation of standardized IQR and waiting time are trivial.

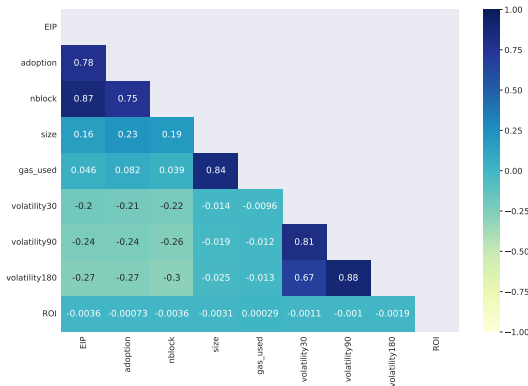


Figure 13: Correlation Heatmap for Control Variables

## C ROBUSTNESS CHECKS

### Fee Dynamics

Table 7 shows that though median gas prices increased overall after London Hardfork without controls, they dropped if controlling time trend and price volatility.

Table 8 displays the regression outcome with standardized IQR as the dependent variable, the indicator variable of London Hardfork and EIP-1559 adoption rate as independent variables. Column (1) displays that the aggregate effect of the network upgrade to the intra-block price variance is negative. Columns (2) - (4), carrying an expanding set of control variables, return a consistent estimate on the immediate and short-term effect of EIP-1559 adoption. As shown, the coefficients in the first row on London Hardfork in Columns (2) - (4) are consistently and significantly positive. In contrast, the coefficients in the second row on EIP-1559 adoption are similarly and significantly negative.

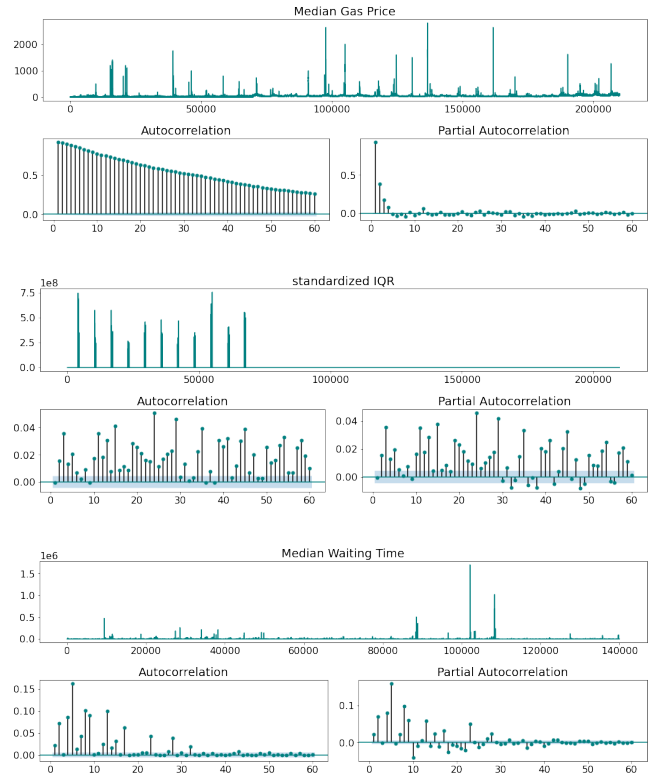


Figure 14: Auto-correlation of median gas price, standardized IQR, and median waiting time

Table 9 shows that though IQR increased immediately after London Hardfork, it dropped significantly and in greater scales in the blocks with more transactions adopting EIP-1559 bidding.

Table 10 shows that our results on standardized IQR are robust to different volatility measures.

### Waiting Time

Table 11 shows that least absolute deviation (LAD) regression results are similar to OLS regressions in Table 2, but the coefficient estimates are overall smaller in scale.

Column (3) in Table 12 shows that transaction type had trivial effects on median waiting time.

## D ADDITIONAL VISUALIZATIONS

Distribution of priority fees in Fig. 15 has two peaks at 2 Gwei and 5 Gwei, with a majority of median priority fee bids under 10 Gwei.

Figure 16 shows the time series of IQR and standardized IQR, the former oscillating with base fee.

Figure 17 shows that the waiting time distribution of legacy and EIP-1559 transactions after London Hardfork, which are similar in general.

Column Name	Source	Annotation
<b>Dataset 1: Block Characteristics</b>		
block_number	BigQuery block data	Block number on blockchain; data key
BQ_timestamp	BigQuery block data	Block timestamp on blockchain
block_hash	BigQuery block data	Hash of the block
sha3_uncles	BigQuery block data	SHA3 of the uncles data in the block
miner	BigQuery block data	miner address
difficulty	BigQuery block data	Integer of the difficulty for this block
size	BigQuery block data	The size of this block in bytes
gas_limit	BigQuery block data	The maximum gas allowed in this block
gas_used	BigQuery block data	The total used gas by all transactions in this block
tr_count	BigQuery block data	Number of all transactions included in this block
base_fee	BigQuery block data	Protocol base fee per gas
<b>Dataset 2: Fee Dynamics</b>		
block_number	BigQuery(BQ) transaction(tx) data	Block number on blockchain; data key
all_gpq[x]	BQ tx data (aggregated on block level)	[x]% quartile of actual gas price paid per gas for all transactions in this block
all_gpcount	BQ tx data (aggregated on block level)	number of transactions with valid gas price paid in this block (= tr_count)
all_prq[x]	BQ tx data (aggregated on block level)	[x]% quartile of priority fee per gas bid by all transactions in this block
all_prcount	BQ tx data (aggregated on block level)	number of transactions with valid priority fee bid in this block (= number of txs that adopt EIP1559 style bid)
all_mfq[x]	BQ tx data (aggregated on block level)	[x]% quartile of max fee per gas bid by all transactions in this block
all_mfcount	BQ tx data (aggregated on block level)	number of txs that adopt EIP1559 style bid
legacy_gpq[x]	BQ tx data (aggregated on block level)	[x]% quartile of actual gas price paid per gas for all transactions that adopts legacy style bid in this block
eip_gpq[x]	BQ tx data (aggregated on block level)	[x]% quartile of actual gas price paid per gas for all transactions that adopts EIP1559 style bid in this block
<b>Dataset 3: Waiting Time</b>		
block_number	Go Ethereum (Geth)	Block number on blockchain; data key
uncle_cnt	Geth	Number of uncles of this block
all_cnt	Geth	Number of all transactions included in this block
all_latetx_cnt	Geth	Number of late transactions in this block
all_nevertx_cnt	Geth	Number of never transactions in this block
all_wtq[x]	Geth	[x]% quartile of waiting time for all transactions included in this block
legacy_cnt	Geth	Number of transactions that adopt legacy bid style included in this block
legacy_latetx_cnt	Geth	Number of late transactions that adopt legacy bid style in this block
legacy_nevertx_cnt	Geth	Number of never transactions that adopt legacy bid style in this block
legacy_wtq[x]	Geth	[x]% quartile of waiting time for transactions that adopt legacy bid style included in this block
eip_cnt	Geth	Number of transactions that adopt EIP-1559 bid style included in this block
eip_latetx_cnt	Geth	Number of late transactions that adopt EIP-1559 bid style in this block
eip_nevertx_cnt	Geth	Number of never transactions that adopt EIP-1559 bid style in this block
eip_wtq[x]	Geth	[x]% quartile of waiting time for transactions that adopt EIP-1559 bid style included in this block
<b>Dataset 4: Miner Extractable Value (MEV)</b>		
block_number	Geth	Block number on blockchain; data key
FBB_coinbase_transfer	Flashbots API	Sum of coinbase transfers of all Flashbot bundles (FBB) transactions in this block
FBB_gas_fee	Flashbots API	Sum of total gas fees paid by all FBB transactions in this block
non_FBB_gas_fee	Geth and Flashbots API	Sum of total gas fees paid to miners (not including burnt fees) by all non-FBB transactions in this block
static_reward	Geth	Static reward to miners in this block
uncle_incl_reward	Geth	Uncle inclusion reward to miners in this block

**Table 5: Data dictionary**

	standardized inter-quartile range			
	(1)	(2)	(3)	(4)
London Hardfork	-0.02509*** (0.00122)	0.08467*** (0.00259)	0.08458*** (0.00260)	0.08603*** (0.00260)
EIP-1559 adoption		-0.24024*** (0.00370)	-0.24191*** (0.00371)	-0.24573*** (0.00374)
nblock		-0.00000*** (0.00000)	-0.00000*** (0.00000)	-0.00000*** (0.00000)
median gas price			-0.00002* (0.00001)	-0.00001 (0.00001)
90-block volatility			-1.66109*** (0.33027)	-1.75653*** (0.33043)
block size				0.00000*** (0.00000)
ROI				1.44643 (1.18377)
Intercept	0.25204*** (0.00088)	0.25896*** (0.00319)	0.27201*** (0.00401)	0.26412*** (0.00413)
Observations	135,757	135,757	135,757	135,756
R <sup>2</sup>	0.00310	0.04446	0.04467	0.04510

Note: Hour fixed effect included. \*p<0.1; \*\*p<0.05; \*\*\*p<0.01

Linear regression with standardized IQR as dependent variable, indicator of London Hardfork and EIP-1559 adoption rate as independent variables, with different sets of controls shown in different columns. Outcome variable data deleted if Q50 gas price < 1 to avoid divided by zero error (standardized IQR = IQR/Q50 gas price). Standard errors are in parentheses. Though standardized IQR increased immediately after London Hardfork, it dropped significantly and in greater scale in the blocks with more transactions adopting EIP-1559 bidding. The long term negative effect outweighs a small short term positive effect. The data frequency is by block. Column (4) is visualized in Fig. 7.

Table 8: Standardized IQR and EIP-1559 Adoption

	Gas Price IQR			
	(1)	(2)	(3)	(4)
London Hardfork	3.48176*** (0.05748)	2.21534*** (0.11910)	2.97793*** (0.11384)	3.03930*** (0.11413)
EIP-1559 adoption		-15.76774*** (0.17052)	-15.11661*** (0.16326)	-15.27582*** (0.16467)
nblock		0.00011*** (0.00000)	0.00008*** (0.00000)	0.00008*** (0.00000)
median gas price			0.07002*** (0.00063)	0.07041*** (0.00063)
90-block volatility			313.22922*** (14.45058)	308.95025*** (14.46024)
block size				0.00000*** (0.00000)
ROI				91.86449* (51.68797)
Intercept	8.94921*** (0.04133)	12.71802*** (0.14698)	6.67830*** (0.17614)	6.34828*** (0.18179)
Observations	137,025	137,025	137,025	137,024
R <sup>2</sup>	0.02566	0.13203	0.21020	0.21053

Note: Hour fixed effect included. \*p<0.1; \*\*p<0.05; \*\*\*p<0.01

Linear regression with gas price IQR as dependent variable, indicator of London Hardfork and EIP-1559 adoption rate as independent variables, with different sets of controls shown in different columns. Standard errors are in parentheses. Though IQR increased immediately after London Hardfork, it dropped significantly and in greater scales in the blocks with more transactions adopting EIP-1559 bidding. The long term negative effect outweighs a small short term positive effect.

Table 9: Intra-block Gas Price Difference and EIP-1559 Adoption - Measured by IQR

	standardized IQR		
	(1)	(2)	(3)
London Hardfork	0.08622*** (0.00260)	0.08603*** (0.00260)	0.08590*** (0.00260)
EIP-1559 adoption	-0.24707*** (0.00374)	-0.24573*** (0.00374)	-0.24471*** (0.00375)
nblock	-0.00000*** (0.00000)	-0.00000*** (0.00000)	-0.00000*** (0.00000)
median gas price	-0.00001 (0.00001)	-0.00001 (0.00001)	-0.00001 (0.00001)
30-block volatility	-4.12185*** (0.38035)		
90-block volatility		-1.75653*** (0.33043)	
180-block volatility			-0.48006** (0.21847)
block size	0.00000*** (0.00000)	0.00000*** (0.00000)	0.00000*** (0.00000)
ROI	1.43331 (1.18338)	1.44643 (1.18377)	1.45417 (1.18388)
Intercept	0.27417*** (0.00400)	0.26412*** (0.00413)	0.25721*** (0.00421)
Observations	135,756	135,756	135,756

Note: Hour fixed effect included. \*p<0.1; \*\*p<0.05; \*\*\*p<0.01

Linear regression with standardized IQR as dependent variable, indicator of London Hardfork and EIP-1559 adoption rate as independent variables, with different price volatility measures shown in different columns. Standard errors are in parentheses. Our results are robust to different volatility measures.

Table 10: Intra-block Gas Price Difference and EIP-1559 Adoption - Different Volatility Measures

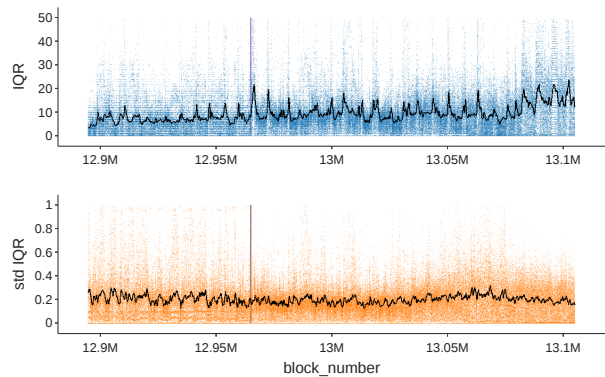
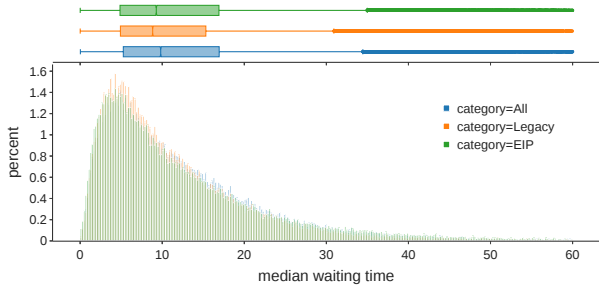


Figure 16: Time Series of intra-block gas price IQR and standardized IQR



**Figure 17: Median waiting time distribution by transaction type after London Hardfork**

Variable Name	ADF Statistics	p-value	Stationary
base fee	-25.65	0.000	Yes
EIP-1559 adoption	-7.58	0.000	Yes
median gas price	-32.92	0.000	Yes
IQR	-29.24	0.000	Yes
standardized IQR	-34.84	0.000	Yes
median waiting time	-60.83	0.000	Yes
90min MA volatility	-10.99	0.000	Yes
block size	-24.50	0.000	Yes
block gas used	-46.85	0.000	Yes

**Table 6: Dickey-Fuller Test for Stationary Variables**

	Median Gas Price		
	(1)	(2)	(3)
London Hardfork	20.2246*** (0.3528)	-11.8181*** (0.7543)	-10.7044*** (0.7509)
EIP-1559 adoption		-0.5387 (1.0776)	-4.7284*** (1.0821)
nblock		0.0005*** (0.0000)	0.0002*** (0.0000)
block size			-0.0001*** (0.0000)
ROI			-76.1414 (343.9860)
90-block volatility			3170.0087*** (89.8447)
Intercept	39.4370*** (0.2492)	55.5752*** (0.3986)	35.6840*** (0.7177)
Observations	138,043	138,043	137,769
R <sup>2</sup>	0.0233	0.0429	0.0684

*Note: Hour fixed effect included* \*p<0.1; \*\*p<0.05; \*\*\*p<0.01  
 Linear regression with block median gas price as dependent variable, indicator of London Hardfork and EIP-1559 adoption rate as independent variables with different sets of controls shown in different columns. Standard errors are in parentheses. Results are mixed: median gas prices increased overall after London Hardfork without controls, but they in fact dropped if controlling time trend and price volatility.

**Table 7: Median Gas Price and EIP-1559 adoption**

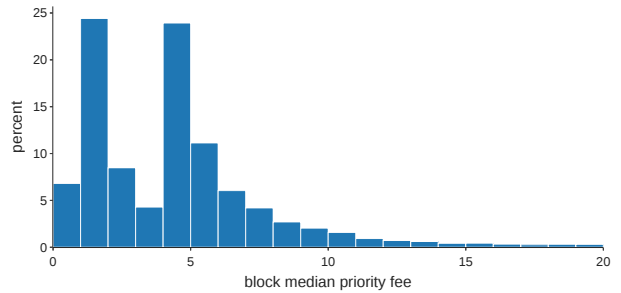


**Figure 15: Distribution of priority fee bid**

	Median Waiting Time			
	(1)	(2)	(3)	(4)
London Hardfork	-6.4660*** (0.07587)	-6.07273*** (0.16333)	-6.18858*** (0.16342)	-3.90310*** (0.09868)
EIP-1559 adoption		-0.94735*** (0.23883)	-1.01186*** (0.23850)	-4.75727*** (0.14501)
nblock		0.00000 (0.00000)	0.00000** (0.00000)	-0.00002*** (0.00000)
median gas price			-0.00650*** (0.00089)	0.00692*** (0.00054)
90-block volatility			0.12689*** (0.00712)	0.01709*** (0.00427)
block size				0.00011*** (0.00000)
ROI				-0.00036*** (0.00003)
Intercept	16.77700*** (0.19032)	16.80625*** (0.20135)	17.15675*** (0.20672)	8.38608*** (0.13158)
Observations	135,513	135,513	135,513	135,512

Note: Hour fixed effect included. \*p<0.1; \*\*p<0.05; \*\*\*p<0.01

Least absolute deviation (LAD) regression with block median waiting time as dependent variable, indicator of London Hardfork and EIP-1559 adoption rate as independent variables with different sets of controls shown in different columns. Standard errors are in parentheses. Results are similar to OLS regressions in Table 2, but the coefficient estimates are overall smaller in scale.

**Table 11: Ethereum Median Waiting Time and EIP-1559 Adoption - LAD Regression**

	Median Waiting Time		
	(1)	(2)	(3)
TxType == 2	-0.49933*** (0.13514)	-1.14876*** (0.12950)	0.00059 (0.00088)
nblock	0.00005*** (0.00000)	0.00001** (0.00000)	
EIP-1559 adoption	-3.83371*** (0.30980)	-9.74894*** (0.30025)	
90-block volatility		59.16974 (37.05756)	
block size		0.00013*** (0.00000)	
ROI		-125.41390*** (36.26787)	
Intercept	14.76364*** (0.15423)	5.37660*** (0.30356)	-0.00345 (0.03561)
Observations	137,780	137,780	140,000
R <sup>2</sup>	0.70541	0.73170	0.00000

\*p<0.1; \*\*p<0.05; \*\*\*p<0.01

Fixed effect regression with median waiting as dependent variable, indicator of transaction type as independent variable, with different sets of controls shown in different columns. Hour fixed effect included in Column (1) and (2), while block fixed effect included in Column (3). Standard errors are in parentheses. Column (3) shows that transaction type had trivial effects on median waiting time.

**Table 12: Comparison of Waiting Time between Legacy Style Transactions and EIP-1559 Style Transactions**